3D evolution of detachment fault systems in necking domains: insights from the Klakk Fault Complex and the Frøya High, mid-Norwegian rifted margin

J. L. S. Gresseth[1,*], P. T. Osmundsen[1, 2], and G. Péron-Pinvidic[1, 3]

[1] Department of Geoscience and Petroleum, Norwegian University of Science and Technology, 7031 Trondheim, Norway

[2] Department of Arctic Geology, University Centre in Svalbard, 9171 Longyearbyen, Norway

[3] Geological Survey of Norway, 7040 Trondheim, Norway

*Corresponding author: Julie L. S. Gresseth (julie.gresseth@ntnu.no)

Key points

- Central parts of the Frøya High in the necking domain of the mid-Norwegian margin represent an eroded turtleback structure
- Evolution of increasingly sinusoidal detachment fault geometries may lead to successive incision, and complex lateral linkage
- Increasingly sinusoidal detachment fault geometries control the spatio-temporal distribution of depocenters throughout fault evolution

Abstract

Detachment fault systems typically record displacements in the order of 10s of kilometers. The principles that control the growth of smaller magnitude normal fault systems are not fully applicable to the evolution of detachment fault systems. We use interpretation of 2D and 3D seismic reflection data from the mid-Norwegian rifted margin to investigate how the structural evolution of a detachment fault interacted with the effects of isostatic rollback to produce complex 3D geometries and control the configuration of associated supradetachment basins. We further investigate the effects of lateral interaction and linkage of extensional detachment faults on the necking domain configuration. In our study area, the domain-bounding Klakk Fault Complex demonstrates how successive incision may induce a complex

structural relief in response to faulting and fault plane folding. We interpret the previously proposed metamorphic core complex within its footwall as an extension-parallel turtleback-structure. The now eroded turtleback is flanked by a major supradetachment basin, connecting two main basin segments. We attribute footwall- and turtleback exhumation to Middle Jurassic - Early Cretaceous rifting. The study area further demonstrates how detachment fault geometries can change during rifting and lead to the formation of younger, successively incising fault splays. Lateral linkage between the original detachment fault plane and these fault splays enables displacement along a detachment fault system consisting of fault segments generated at different stages in time. Implicitly, detachment faults are complex 3D systems that change configuration during their evolution, perpetually controlling associated basin formation, footwall configuration and uplift patterns.

1. Introduction

An increased focus on rifting processes and continental margin formation in recent years has inspired a string of concepts and definitions for rifts and rifted margins. Seminal discoveries include the subdivision of many rifted margins into distinct domains (proximal, necking, distal and outer domain), that share fundamental structural-morphological characteristics (Chenin et al., 2017; Manatschal, 2004; Osmundsen & Péron-Pinvidic, 2018; Péron-Pinvidic et al., 2013; Peron-Pinvidic et al., 2019; Ribes et al., 2019; Sutra et al., 2013). A related concept is the bounding of these domains by breakaway complexes (Osmundsen & Péron-Pinvidic, 2018) (Figure 1). These specific structures are identified as large-scale, complex fault systems that develop sequentially seaward as rifting progresses. Although several studies address the successive, down-dip evolution of such breakaway complexes, their nature in terms of nucleation, lateral growth, displacement, and interaction remains poorly understood.

Seaward from the innermost proximal domain is, conceptually, the necking domain, delineated by the necking breakaway complex(es) (e.g., Osmundsen & Péron-Pinvidic, 2018; Péron-Pinvidic et al., 2013) (Figure 1e). The necking domain corresponds to the area where the crust becomes wedge-shaped and the crustal thickness becomes reduced from ~30 km to < 10 km along large-scale detachment faults (Péron-Pinvidic & Manatschal, 2009; Péron-Pinvidic et al., 2013). The domain thus involves a drastic bulk increase in accommodation space, and was suggested by Tasrianto and Escalona (2015) to delineate the most hydrocarbon-prospective segments of rifted margins.

The inner necking breakaway complex normally entails abrupt, but moderate increase in accommodation with large, basinward dipping normal faults incising into ductile middle crust. It defines the boundary between the moderately thinned proximal domain and the more highly extended necking domain. The outer necking breakaway complex is defined by the first fault that cuts the middle crust and continues into lower crust and upper mantle (Osmundsen & Péron-Pinvidic, 2018). The outer necking breakaway complex delineates necking domains (e.g., Chenin et al., 2017; Sutra et al., 2013), as it commonly defines a megafault scarp (Ribes et al., 2019) and the associated wedge-shaped crustal geometry is easily recognized, even in areas of poor data quality and coverage. It commonly shapes the crustal taper and, eventually, the taper break (Osmundsen & Redfield, 2011), where crustal thickness is reduced to 10 km or less. Conceptually, the outer parts of the necking domain correspond to the area where the first brittle faults crosscut the entire crust and penetrate the mantle (Osmundsen & Péron-Pinvidic, 2018; Péron-Pinvidic et al., 2013), and the taper break commonly connects their hanging wall cutoffs towards the first rotated fault-block in the hyperextended distal margin (Figure 1e).

Several rifted margin studies include constraints on the necking domain, examples from conjugate rifted margin systems include the Western Iberia and Newfoundland margins (Mohn et al., 2015; Péron-Pinvidic et al., 2013; Sutra & Manatschal, 2012; Sutra et al., 2013); the mid-Norway – East Greenland margins (Osmundsen & Péron-Pinvidic, 2018; Péron-Pinvidic et al., 2013) and the East Africa – Brazilian rifted margins (Blaich et al., 2011; Zalán et al., 2011). Furthermore, necking domains have also been described from the Bay of Biscay (Tugend et al., 2015), the Gulf of Aden (Nonn et al., 2017), on the northwestern Adriatic margin preserved in the Central Alps (Ribes et al., 2019), the Labrador Sea (Gouiza & Naliboff, 2021), the Baffin Bay (Welford et al., 2018), and the Irish margins (Lymer et al., 2019; Welford et al., 2010).

In combination with large displacement magnitudes, the formation of core complexes and basement culminations in the footwalls of necking breakaway complexes effectively sets up configurations ideal for establishing supradetachment basins in the hangingwall. Friedmann and Burbank (1995) introduced the term ‘supradetachment basin’ based on the juxtaposition of such basins with extensional detachment faults. They interpreted supradetachment basins to record significantly higher magnitudes of crustal extension than predicted by traditional models for rift systems. This would lead to categorical variations in bounding fault dips and displacements, stretching factors, rates of uplift/subsidence, drainage style and sedimentary architecture, either compliant with rift- or supradetachment basin style (Friedmann & Burbank, 1995; Serck et al., 2021). Rift basins (e.g., Gawthorpe et al., 1994; Henstra et al., 2017) and supradetachment basins are described in literature with fewer, yet well-known cases of the latter found in e.g. the North Atlantic margin (Osmundsen & Péron-Pinvidic, 2018), the Scandinavian Caledonides (e.g., Braathen et al., 2002; Osmundsen & Andersen, 2001; Seranne, 1992; Vetti & Fossen, 2012), Tibet (Kapp et al., 2008), pre-Basin and Range in the western US (e.g., Friedmann & Burbank, 1995) and Oman (Serck et al., 2021). A supradetachment basin was recently described within the necking domain of the mid-Norwegian Rifted margin (Muñoz-Barrera et al., 2020).

With very few notable exceptions (e.g., Lymer et al., 2019), studies of the deep structure of rifted margins have mostly been based on spaced long-offset 2D seismic reflection lines (e.g., Faleide et al., 2008; Manatschal, 2004; Osmundsen & Péron-Pinvidic, 2018; Péron-Pinvidic et al., 2013; Sutra et al., 2013; Zastrozhnov et al., 2020), and have resulted in models that are essentially 2D or 2,5D. Previous studies indicate that significant structural and geomorphological variability occurs over relatively small distances along-strike, thus calling for investigating the nature of these systems in 3D and to resolve their evolution in 4D. The necking domain of the mid-Norwegian is densely covered by high-resolution 2D and 3D seismic reflection data, and reportedly contains numerous extensional detachment faults and buried megafault scarps (Bunkholt et al., 2021; Muñoz-Barrera et al., 2020; Osmundsen & Péron-Pinvidic, 2018; Osmundsen et al., 2021). The area thus exhibits the perfect laboratory for investigating the interplay between tectonic rifting processes and supradetachment basin evolution along the extent of the necking domain.

Our study focuses on the necking domain of the Vøring segment of the mid-Norwegian rifted margin where the large-scale, domain-bounding Klakk Fault Complex (KFC) constrains the Frøya High in its footwall from the Rås Basin in its hangingwall (Figure 1). The study area reveals how significant spatio-temporal variations along-strike of the KFC reflect a continuously reiterating detachment fault system. The KFC consists of a major detachment fault segment partly reactivated and partly incised by more minor, individual segments generated at various stages throughout the evolution of the detachment fault system. We find that a complex interplay between localized isostatic uplift, successive incision and lateral linkage over time produced a footwall turtleback structure flanked by a supradetachment basin in its hangingwall. Implicitly, this work introduces a new evolutionary model for the KFC of likely significant relevance for understanding 4D necking domain evolution world-wide.

2. Geological Framework

2.1 Regional tectonics

The structural framework of the mid-Norwegian margin was largely defined by Blystad et al. (1995) and is, along with adjacent land areas, well-covered in literature (e.g., Blystad et al., 1995; Braathen et al., 2002; Bunkholt et al., 2021; Corfu et al., 2014; Doré et al., 1999; Fossen, 2010; Muñoz-Barrera et al., 2020; Osmundsen & Péron-Pinvidic, 2018; Osmundsen et al., 2021; Osmundsen et al., 2002; Redfield et al., 2005; Zastrozhnov et al., 2020). The processes that structured the continental margin can be grouped into three principal phases spanning in time from the Mid Paleozoic until present (e.g., Blystad et al., 1995); compression, episodic extension, and continental drift.

During the Late Silurian-Early Devonian, the continent-continent collision between Laurentia and Baltica closed the proto-Atlantic Iapetus Ocean and resulted in the Caledonian orogeny (Corfu et al., 2014; Gee et al., 2013). The now deeply eroded mountain chain featured major thrust and nappe units with an overall E to SE vergence (Corfu et al., 2014; Seranne, 1992). Onshore Norway, many of the compressional structures are overprinted by extensional shear zones as in e.g., Southwestern (Andersen & Jamtveit, 1990; Krabbendam & Dewey, 1998; Osmundsen & Andersen, 2001), and Central Norway (Braathen et al., 2002; Osmundsen et al., 2006). Devonian extensional shear zones were superimposed on Caledonian nappe stacks, where extensional structures are attributed to reactivation of low-angle Caledonian thrusts as well as initiation of incising normal faults, reflecting extensional collapse of the orogen from 403 to 380 Ma (Braathen et al., 2002; Dunlap & Fossen, 1998; Fossen, 2010; Osmundsen et al., 2006).

In the Lower to Middle Devonian, a complex interplay between extension and strike-slip movements led to formation of a series of extensional detachments and shear zones that bound an array of intra-montane Devonian basins along the Norwegian margin (Andersen &

Jamtveit, 1990; Braathen et al., 2004; Braathen et al., 2002; Corfu et al., 2014; Lenhart et al., 2019; Osmundsen & Andersen, 2001; Osmundsen et al., 2006; Seranne, 1992). The basins bound by major detachments and associated shear zones were formed under regional transtension, and thus under constrictional strain leading to their elongated, extension-parallel geometry (Braathen et al., 2002; Krabbendam & Dewey, 1998; Osmundsen & Andersen, 2001; Osmundsen et al., 2006). Pertinent examples of these detachment systems are the Nordfjord-Sogn Detachment Zone (NSDZ) in the Western Gneiss Region (WGR) in Southwestern Norway, and the Høybakken Detachment (HDZ) in Central Norway (e.g., Braathen et al., 2002; Norton, 1986). The Southwestern and Central segments of the Scandinavian Caledonides in Norway are separated by the ENE striking Møre Trøndelag Fault Complex (MTFC). The MTFC represents a reactivated fault zone with a geological history recording orogeny, subsequent collapse and rift-to post-rift reactivation from Paleozoic through Cenozoic times (Corfu et al., 2014; Gabrielsen et al., 1999; Osmundsen et al., 2021; Redfield et al., 2005; Redfield et al., 2004; Seranne, 1992).

2.1.1 Main phases of deformation

Repeated extensional deformation followed from Late Devonian times with pronounced rifting events in Late-Permian-Early Triassic, late Middle Jurassic-Early Cretaceous, and Late Cretaceous-Early Paleogene times (Blystad et al., 1995; Osmundsen et al., 2021). This multi-phase rifting led to the formation of a systematic oceanward succession of key structural domains within the mid-Norwegian rifted margin. Following the principles of Lavier and Manatschal (2006) and Péron-Pinvidic et al. (2013), these domains reflect the interaction of four deformation phases along the margin; stretching, thinning and hyper-extension (-exhumation), followed by final breakup and oceanization.

The *stretching phase* included mild rifting in the mid-Carboniferous followed by extensive block faulting during Late Permian-Early Triassic times (Blystad et al., 1995; Bunkholt et al., 2021; Muñoz-Barrera et al., 2020; Péron-Pinvidic et al., 2013). This phase created half-grabens as well as supradetachment basins. Evidence for substantial crustal thinning has been found in the NNE and NE-striking Helgeland and Froan Basins in the proximal domain, showing that the formerly presented moderate ‘stretching phase’ is more complex than assumed previously, involving large magnitudes of extension and very deep basins (Osmundsen & Péron-Pinvidic, 2018; Osmundsen et al., 2021; Peron-Pinvidic et al., 2020).

The following *thinning phase* involved mild rifting during the Early Jurassic focused mainly on the Halten Terrace, and more significant rifting during latest Middle to Late Jurassic between the Trøndelag Platform and the Rås and Træna basins, and the narrow platform in the Møre area and the Slørebotn Subbasin (Bunkholt et al., 2021; Osmundsen et al., 2021; Peron-Pinvidic et al., 2020). The margin's necking domain was established during this phase with the large-scale Main Møre boundary fault and the Klakk, Bremstein, Ytreholmen and Vingleia Fault Complexes (Blystad et al., 1995; Bunkholt et al., 2021; Muñoz-Barrera et al., 2020; Osmundsen & Ebbing, 2008; Osmundsen et al., 2021).

The third phase of rifting, the *hyperextension (-exhumation) phase* initiated as a major rifting episode during earliest Cretaceous and a less extensive rift phase during middle Cretaceous (Blystad et al., 1995; Osmundsen & Péron-Pinvidic, 2018). Extensional deformation focused in the Rås basin, creating hyperextended and sag basins (Osmundsen & Péron-Pinvidic, 2018; Péron-Pinvidic et al., 2013).

During the fourth rifting phase in the Late Cretaceous, extension localized mainly in the distal domain, producing the Møre and Vøring marginal highs. It culminated in the continental separation between Eurasia and Greenland in the earliest Eocene (Blystad et al., 1995; Faleide et al., 2008; Zastrozhnov et al., 2020). Following the continental break-up and onset of seafloor spreading in the North Atlantic Ocean, continental drift continued and is presently represented by the active mid-Atlantic spreading ridge (Blystad et al., 1995; Lien, 2005). Thermal subsidence since the Early Cretaceous has over time produced the margin's current down-to-the west tilt (Bunkholt et al., 2021; Faleide et al., 2008).

2.2 Study area

This study focuses on the margin's necking domain-bounding KFC, which separates the Frøya High and Sklinna Ridge in its footwall from the Rås basin in its hangingwall (Figure 1) (Blystad et al., 1995; Bunkholt et al., 2021; Muñoz-Barrera et al., 2020; Osmundsen & Péron-Pinvidic, 2018). The westward-dipping KFC presents a c. 270 km long, 10-15 km wide, partly eroded escarpment zone. The escarpment zone consists of complex faults and erosional surfaces along the western margins of the Frøya High and Sklinna Ridge (Bunkholt et al., 2021; Muñoz-Barrera et al., 2020).

A total of seven (semi-)regional unconformities have been mapped on the mid-Norwegian margin, of which three – the Callovian-Oxfordian Intra Melke Unconformity

(IMU), the Tithonian-Berriasian Base Cretaceous Unconformity (BCU) and the late Early Cretaceous Base Cenomanian Unconformity (BCenU) – are documented and constrained by well data within the study area (Bunkholt et al., 2021). Seismic data reveal confidently mappable heaves of 20-35 km along the KFC (Muñoz-Barrera et al., 2020; Osmundsen & Péron-Pinvidic, 2018), effectively displacing the BCU down to its deepest structural level in the area to 9.5 s TWT (Bunkholt et al., 2021). According to Osmundsen and Péron-Pinvidic (2018) the KFC represents a combined inner and outer necking breakaway complex along the Frøya High, with significant spatio-temporal variations in geometry and crustal thinning (Figure 1d).

In the south, the KFC interacts with the Jan Mayen Lineament (JML) and the MTFC. The sinistral, transform fault system of the NW-SE trending JML separates the Møre and Vøring Basins (Blystad et al., 1995). Albeit the JML serves as a regionally important structural boundary, there appears to be little evidence in the seismic data to suggest that JML exerted control on the structuring and evolution of the KFC (Muñoz-Barrera et al., 2022; Muñoz-Barrera et al., 2020). The influence exerted by the MTFC is, however subject of ongoing debate but is assumed to have been significant (Gabrielsen et al., 1999; Osmundsen & Péron-Pinvidic, 2018). The ENE-striking and 750 km long, down-to-the-NW MTFC separates the northern North Sea from the Møre Margin (Gabrielsen et al., 1999), and is composed of several fault segments in an up to zone up to c. 80 km wide (Muñoz-Barrera et al., 2020). Osmundsen and Péron-Pinvidic (2018) define the southeastern strand of the MTFC in the Møre margin segment as a proximal breakaway complex, whereas the northwestern strand comprises the outer necking breakaway complex in the form of the Main Møre boundary fault. The MTFC has been interpreted to have facilitated dextral movement during the Silurian (Seranne, 1992), sinistral movement during the Devonian (Osmundsen et al., 2006; Seranne, 1992), and several brittle dip-slip to oblique-slip and dextral displacement events since the late Paleozoic (Gabrielsen et al., 2002; Grønlie & Roberts, 1989; Redfield et al., 2005; Redfield et al., 2004).

The KFC interacts northwards with the N-S and NE-SW striking Bremstein and Vingleia Fault Complexes (BFC and VFC, respectively, Figure 1). The latter separates the Frøya High from the southern Halten Terrace, before it, according to Bunkholt et al. (2021) joins the Bremstein Fault Complex (BFC) trending directly north. Major displacements occurred along these fault complexes during the stretching phase, effectively dissecting the sedimentary fill into several discrete (minor) structural elements (e.g., horsts, graben, and rotated fault blocks) (Bell et al., 2014; Bunkholt et al., 2021).

In the footwalls of the main detachment systems, wells 6306/10-1, 6407/10-3, 6306/6-1, and 6306/6-2 (red circles on Figure 1c) penetrate basement lithologies on the Frøya High and Gossa Highs, composed by baltic granite and gneiss (NPD, 2022). The most detailed reports of basement lithologies are found in well 6306/10-1 on the Gossa High (Figure 1c). The well drilled 207 meters of fractured and altered gneissic basement, where Rb-Sr dating of material within the weathered section yielded Early Carboniferous age (335 Ma). The upper 30 meters of the basement section are described as rich in kaolinite and severely weathered (NPD, 2022).

Muñoz-Barrera et al. (2022) presented a qualitative analysis of the supradetachment basin segment situated between the Frøya and Gossa highs, bound by the KFC and the Main Møre boundary fault. They mapped three megasequences and inferred their ages based on megasequence morphology and known geological setting. The supradetachment basin was mapped to have a spoon-shaped geometry with a WNW-ESE axis orientation, and interpreted to constrain; 1) pre-thinning phase sediments in Middle Triassic to Early Jurassic, 2) syn-rift deposits during Early Jurassic to Early Cretaceous times, and 3) post-rift sediments following Early Cretaceous times (Muñoz-Barrera et al., 2022).

3 Data and Methods

The seismic reflection data used in this study includes three 3D seismic surveys and a suite of 2D lines from both regional and local seismic surveys (Figure 1c). Conventional seismic interpretation was performed using the Schlumberger Petrel 2020® seismic interpretation software. The results of the seismic interpretation were correlated with potential field data maps from Olesen et al. (2010a); Olesen et al. (2010b) and data from a total of twelve exploration wells, of which four are considered key wells; 6306/10-1, 6306/6-1, 6306/6-2, 6407/10-3 (Figure 1 c). The recorded depth of the seismic surveys varies from five to twelve s TWT (seconds two-way time). Seismic reflection data were processed in zero-phase and are displayed according to the Society of Exploration Geophysicists (SEG) reverse polarity convention, i.e., peaks (blue) indicate a downward increase in acoustic impedance, whilst troughs (brown) represent a downward decrease in acoustic impedance. Intrabasement seismic facies characteristics and have been analyzed following a workflow like those outlined in recent papers by e.g., Fazlikhani et al. (2017); Gresseth et al. (2022); Lenhart et al. (2019); Phillips et al. (2016); Muñoz-Barrera et al. (2020) and Wiest et al. (2020), where constraining facies units and truncating relationships locate tectonic boundaries.

4 Results and observations

4.1 The Klakk Fault Complex

On a margin scale, the KFC separates the Frøya High and the Sklinna Ridge from the Rås basin in the northern Møre and southern Vøring Basin segments, before the Ytreholmen FC forms the eastern limitation of the Rås Basin in the central Vøring Basin (Figure 1). Our study extends over a corridor where KFC constrains the Frøya High from the Rås Basin (Figure 1). The extension facilitated by the KFC along the Frøya High is dispersed across several fault complexes including the northwards continuation of the KFC north of the high, the Bremstein, Vingleia, Revfallet Fault Complexes and associated subsidiary fault sets (Figure 1b). These faults effectively compartmentalized the different segments of the Dønna and Halten Terraces during the margins thinning phase (Bell et al., 2014), whilst the same strain was mainly facilitated solemnly by the KFC along the Frøya High.

The KFC exhibits significant along-strike structural variation within the study area, both in terms of strike, displacement, and magnitude (Figures 3 and 3). Along-strike, the sinuous shape of the KFC set up a configuration where a structural footwall salient is bordering two structural recesses, one to the north and one to the south (Figure 2). The KFC thus differs from standard normal fault configurations which forms relatively straight lineaments oriented perpendicular to the direction of extension. Down-dip its main strand, the KFC exhibits listric geometries with decreasing dip with depth. Measured heaves of top basement cut-offs range from about 15 to 35 km: 31,3 km in the northern structural recess, 18,4 km in the central salient, and 28,3 km in the southern structural recess (Figure 3). Depth conversion of seismic sections has not been performed for this study, but reportedly displacements range from c. 20-40 km and dip generally decreases from ca. 54° ± 9°, to 12° ± 4° at c. 14 km depth based on depth-converted sections (Muñoz-Barrera et al., 2022; Table 4 in Muñoz-Barrera et al., 2020)

4.1.1 The northern structural recess

In the northern structural recess, the KFC exhibits multiple fault-segments (Figure 4). The main strand of the KFC and the western fault segment link at c. 6,5 s TWT depth when viewed in in downdip section (Figure 3a), and envelope a lozenge-shaped fault block. The hanging-wall basin associated with the fault block contains pre-Late Jurassic sediments constrained by well 6306/5-2 (Figure 4). Cretaceous strata onlap the western fault segment. Implicitly, the western fault strand of the KFC is younger than its eastern predecessor and represent successive incision basinward. Laterally, in the north, the fault strands link at the transition between the Frøya High and the Halten Terrace and in the south they link in the central part of the Frøya High (Figure 2 and 4). The area thus evidence both downdip successive incision basinward and fault linkage along strike. In the northern structural recess, the KFC consists of fault segments of different ages, reflecting various stages in the KFC evolution.

4.1.2 The central salient

Where outlining the central salient of the Frøya High, the KFC is represented by a severely eroded fault scarp down to about 5,5 s TWT, below which the listric nature of the KFC is preserved (Figure 3b). At shallower levels however, the fault scarp is locally eroded by incising valleys obscuring the fault plane geometry prior to erosion. Overall, the remnant fault scarp exhibits a convex upwards shape in cross-section (Figure 3b) (also in depth converted sections (Muñoz-Barrera et al., 2020: Figure 5)), and a sinusoidal shape visible in map view (Figure 2). The fault geometry and radial erosional pattern outlines the central salient as a rounded feature in map view, with a salient width of c. 45 km at its widest measured parallel to the overall NNE-SSW trend of the KFC (Figure 2).

4.1.3 The southern structural recess

In the southern structural recess, rotated fault blocks capped by pre-Cretaceous strata rest at higher crustal levels east of the KFC fault segment separating the Frøya High from the Rås Basin (Figure 3c). Whilst different fault segments of the KFC link in the northern structural recess, the southern structural recess exhibits how the KFC partly reactivates and incises the sub-horizontal Slørebotn Detachment along NW-SE transects. The KFC merges with the ENE-SSW Main Møre boundary fault, the outer strand of the MTFC (Figures 1 and 2), effectively documenting the offshore continuation of the MTFC trend in the southernmost part of the study area.

The sinusoidal geometry of the KFC strongly contrasts the NNE-SSW trending fault which constrains the Holmen High (Figure 2). The fault forms the southern continuation of the fault segment that separates the Sklinna Ridge from the Rås basin adjacent the Halten Terrace. Where separating the Sklinna Ridge from the Rås basin, this fault segment is also termed as the KFC according to published literature (e.g., Blystad et al., 1995). No evidence of hard linking between the KFC within the study area and the western boundary of the Sklinna Ridge has been observed in seismic data for this study. Notably, however, the fault constraining the Holmen High incises the flank of the Slørebotn Subbasin in the southern structural recess, indicating that this relatively straight fault segment is younger than the sinusoidal KFC (Figure 2).

4.2 Footwall configuration: Frøya High

In terms of intrabasement seismic facies, differentiable zones with specific reflection characteristics occur within the Frøya High. Detailed intrabasement seismic facies analysis within the high is largely beyond the scope of this study (readers are referred to e.g., Muñoz-Barrera et al., 2020) but we do identify two main zones of high-frequency, parallel-dipping reflector packages interpreted to represent distinct seismic facies (SF); SF1 and SF2 (Figure 3). SF1 only occurs in immediate proximity to KFC in seismic cross-sections. The true structural thickness of SF1 decreases where incising valleys erode the fault scarp, indicating that SF1 was established prior to the current observable erosion pattern. At depth, SF1 merges into the KFC, and partly overprints the second band of intrabasement seismic reflectors; SF2. SF2 is observed within the Frøya High, and only occurs in immediate proximity to KFC where the KFC soles out onto reflectors associated with SF2 at depths of 7 to 10 s TWT. Relative to SF1, SF2 exhibits higher amplitudes and more continuous reflectors. Whilst the eastern extent of the SF1 is within the Frøya High, 2D seismic line coverage suggests that SF2 has an eastern continuation beyond the seismic data coverage with sufficient resolution at depth to be displayed for the Frøya High.

The geomorphology of the top basement surface across the Frøya High is characterized by two main knick-zone lineaments are traceable across the high with an overall NNE-SSW trend (Figure 5). Implicitly, these lineaments follow the along-strike trend of the KFC and delineate three distinct morphological footwall segments A-C, separated by their different dips (Figure 5). Seismic-to-well-ties with wells 6306/6-1, 6306/10-1, and 6407/10-3 (Figure 1c), suggest that surfaces A-C represent erosional unconformities of Mid-Cretaceous, late Middle Jurassic and pre-Triassic ages, respectively. The different ages of the erosional surfaces indicate varying source-to-sink relationships, likely corresponding to distinct footwall configurations influenced by discrete climatic and environmental scenarios through time. Assuming erosion occurred semi-horizontally, the differential dips between the surfaces thus reflects individual magnitudes of footwall backrotation during footwall uplift.

4.3 Hangingwall supradetachment configuration: Rås Basin

The central part of the Frøya High is flanked by a supradetachment basin with two synclinal depocenters in the northern and southern structural recesses, evident in both seismic sections and in plain view (Figures 2, 3 and 5). The supradetachment basin capped by the BCU in the southern structural recess is traceable on 2D seismic lines around the high and into the northern structural recess (Figure 3). This observation effectively correlates the main basin segments into one major supradetachment basin flanking the central salient. The degraded footwall functioned as main source area for the supradetachment basin, evident from the deeply incising valleys representing transport pathways for footwall erosional products (Figures 2 and 5), particularly well displayed around the central salient. Our observations align with the inferred dating of three megasequences suggested by Muñoz-Barrera et al. (2022); Middle Triassic to Early Jurassic pre-rift deposits, overlain by syn-tectonic deposits of likely Early Jurassic to Early Cretaceous age, followed by post-rift sediments after Early Cretaceous times.

4.4 Potential field data correlation maps

The top metamorphic basement surface as mapped based on seismic reflection data largely corresponds to high gravity anomalies within the study area (c. 60 mGal) (Figures 2 and 6a). High positive gravity anomalies are recorded above the central structural salient, following the sinusoidal geometry of the KFC westward. Gravity anomalies of similar magnitude are recorded also for the Gossa High (c. 60 mGal) and east of the Slørebotn Subbasin (c. 70 mGal) (Figure 6). As for the magnetic anomaly response, high positive magnetic anomaly values are largely consistent for the extent of the Frøya High, the highest anomaly values being recorded east of the northern structural recess (c. 500 nT) (Figure 6b). Other notable high positive magnetic anomaly values are located east of the Slørebotn Subbasin (c. 300 nT), east of the VFC (c. 400 nT), in the central part of the Froan basin and in the Proterozoic crystalline rocks in the footwall of the HD onshore (c. 500 nT). The areal distribution of the KFC does not spatially coincide with high positive magnetic anomalies in the central structural salient. Notably, the Gossa High, previously identified as a metamorphic core complex (Osmundsen & Péron-Pinvidic, 2018) exhibits relatively low positive magnetic anomalies (c. 10 nT). Figure 6c exhibits a time-structure map for Top SF2, the reflector band corresponding to the candidate for the offshore continuation of the Høybakken Detachment (HD), also marked in blue in Figure 3. The intrabasement HD reflectors are traceable in close to the entire study area and exhibit a hyperbolic shape when displayed in map view (Figure 6c), and coincide with the Slørebotn detachment below the Slørebotn Subbasin east of the Gossa High. The domal shape of the HD reaches the shallowest crustal levels just north of the central salient of the Frøya High and rests at significantly higher crustal levels within the footwall of the Frøya High, relative to the Rås Basin (Figure 6c). Also, it reaches its shallowest levels just east of the northern structural recess where positive magnetic anomalies reach its highest values (c. 500 nT). The correlation between the positive magnetic anomalies and the top candidate for the HD (Figure 6) indicate that the magnetic anomalies reflect the offshore continuation of crustal materials capped by the HD, as observed onshore in the Fosen area (Figure 6b), and documented elsewhere on the shelf (e.g., WGR region; Braathen et al., 2000).

5 Discussion

Sinusoidal detachment faults enveloping core complexes with rocks exhumed from the middle crust, lower crust or upper mantle have been reported world-wide, from continental as well as oceanic realms, e.g. Western US (e.g., Friedmann & Burbank, 1995; Lister & Davis, 1989), the Aegean (Jolivet et al., 2013; Lister et al., 1984a), Himalaya-Tibet (Kapp et al., 2008), West Antarctica (Richard et al., 1994), the Norwegian Caledonides (e.g., Braathen et al., 2004; Osmundsen et al., 2003; Osmundsen et al., 2006), on the Norwegian Continental Shelf (Gresseth et al., 2022; Muñoz-Barrera et al., 2020; Serck et al., 2022), West of Ireland (Lymer et al., 2019) and in the central mid-Atlantic (Escartín et al., 2017). Despite pervasive reports of such observations, several candidates for explaining their origins exists, and lend different weighting to controlling factors. These factors include structural inheritance, crustal rheology, the effects of rift domain inheritance, fault linkage both laterally and vertically, crustal elastic rebound and isostatic compensation, strain field development, strain rate, geothermal gradients and magmatic input into the system (Mohn et al., 2012; Mortimer et al., 2020; Osmundsen & Péron-Pinvidic, 2018; Péron-Pinvidic et al., 2013; Ribes et al., 2019; Sutra et al., 2013; Tugend et al., 2015; Whitney et al., 2013). The interaction, feedback effects and co-dependance of variables and processes for sinusoidal detachment systems in general are beyond the scope of this study. However, we propose that the KFC's sinusoidal geometry and amount of displacement (20 – 40 km) in combination with the hanging-, and footwall configuration are indicative of a turtleback structure scenario. This implies that the Frøya High contains remnants of an exhumed turtleback structure, galvanized by how the KFC functioned as both an inner and outer necking breakaway complex in the study area. In the following, we discuss how our observations indicate an evolution which is both structurally complex, multi-stage and has, to varying degree along strike, been influenced by structural inheritance, localized isostatic uplift, elastic rebound, fault linkage and successive incision.

5.1 Southern Mid-Norwegian margin necking domain evolution

In terms of explaining the evolution of rifts and rift margin architecture, structural inheritance and associated pre-rift rheological heterogeneities are commonly invoked as many margins develop along former orogens (Doré et al., 1997; Gouiza & Naliboff, 2021; Osmundsen et al., 2002; Péron-Pinvidic et al., 2013). Extension rate, initial crustal strength (i.e., composition and temperature), thickness, geothermal gradient, and the competition between frictional and viscous strain (i.e., decoupling vs. coupling) dictate the nature and timing of the tectonic processes that control lithospheric thinning (e.g., Doré et al., 1997; Gouiza & Naliboff, 2021; Osmundsen et al., 2002; Péron-Pinvidic et al., 2013). These parameters, in combination with local rheological patterns highly influence along-strike rift evolution within each specific rift domain (Gouiza & Naliboff, 2021; Osmundsen & Péron-Pinvidic, 2018; Péron-Pinvidic et al., 2013). Several studies of rifted margins have argued that the oceanward progression of successive stages of crustal thinning is associated with a lowering of the ductile-brittle transition (Sutra & Manatschal, 2012). Each successive breakaway complex may produce prominent footwall culminations as responses to footwall exhumation if the detachment fault system reaches the adequate amount of displacement (Péron-Pinvidic et al., 2022a). This may also entail a down-stepping of the crustal level at which the formation of culminations and core complexes occurs as deformation migrates seawards in rifted margins (e.g., profiles in

Péron-Pinvidic et al., 2022b). Accordingly, for the mid-Norwegian rifted margin, the footwall culminations associated with the proximal domain in the e.g., Froan Basin resides at higher crustal levels than those associated with the necking domain and the Frøya High (Figure 1).

Recently published numerical modeling results for rifted margins yield abrupt necking zones over a relatively short distance (c. 100 km), including upwelling of middle to lower crustal material and significant amounts of erosion (Péron-Pinvidic et al., 2022a). Sophisticated modeling techniques in combination with traditional seismic interpretation has led to a recent and still ongoing increase in our understanding of the evolution of rifted margins. The resultant published models (e.g., Péron-Pinvidic et al., 2022a; Peron-Pinvidic et al., 2019; Peron-Pinvidic et al., 2020; Péron-Pinvidic et al., 2022b) also show an increasing structural complexity and variability in rifted margin architecture compared to previous models, e.g., Osmundsen and Péron-Pinvidic (2018) and Péron-Pinvidic et al. (2013). According to Péron-Pinvidic et al. (2022a), models that consider pre-rift orogenic inheritance produce results more in concert with natural observations, thus honoring rheological heterogeneity and structural inheritance as key parameters. On a margin scale, including the tectonic history of the mid-Norwegian margin going back to the Ordovician-Silurian Caledonian orogeny, the modeling results were in greater concert with present day configuration (Péron-Pinvidic et al., 2022a). By definition, the KFC is attributed to middle Jurassic-Early Cretaceous rifting (e.g., Blystad et al., 1995). However, the structural template in which it developed has knowingly been influenced by structures inherited from the Caledonian orogeny, and subsequent orogenic collapse (e.g., Osmundsen et al., 2021). The remnant evidence of this relating to the KFC is expressed in the footwall of the Frøya High, exhibiting seismic reflection patterns likely established prior to main Mesozoic rifting events.

In concert with Muñoz-Barrera et al. (2020) and other recent papers that identify parallel, high-frequency seismic reflectors underlying large-scale faults as shear zones/mylonitic fabrics (Fazlikhani et al., 2017; Gresseth et al., 2022; Lenhart et al., 2019; Phillips et al., 2016; Serck et al., 2022; Strugale et al., 2021), we interpret SF1 and SF2 to represent shear zone fabrics (Figure 3). We interpret SF1 to represent shear fabrics related to the development of the KFC, here on out informally referred to as the Klakk shear zone (Ksz). The Ksz is observed with varying vertical thickness along the KFC fault scarp. The thickness variation observably coincides with the amount of fault scarp degradation on the Frøya High; being the thinnest below incised valleys and thicker where larger amounts of the footwall remain preserved. As such, the Ksz developed during displacement along the KFC and has later been subjected to local erosion with incising valleys degrading the footwall. Elsewhere on the Norwegian continental shelf, several studies have documented tens of kilometers offshore continuation of corresponding Devonian shear zones further south: NSDZ; ~ 60 km (Lenhart et al., 2019); KSZ and SSZ: ~ 50 km; HSZ: ~70 km (Fazlikhani et al., 2017; Lenhart et al., 2019; Phillips et al., 2016; Wiest et al., 2020). The KFC soles out onto, and partly merges with SF2 at depth. Based on its structural relation to the KFC, its relative magnitude and westerly position ~ 120 km of the Høybakken Detachment onshore, we suggest that SF2 represents the offshore continuation of the Høybakken Detachment (Figures 1, 3 and 6c). SF2 will in the following informally be referred to as the Høybakken Detachment shear zone (HDsz).

The Ksz seems to partly merge with and overprint the interpreted HDsz (Figure 3). This likely represents partial reactivation of the Devonian structural template during late Middle Jurassic - Early Cretaceous rifting. Péron-Pinvidic et al. (2022a) pointed out that the pre-rift structural template within necking domains may only partly be exploited. Ksz merging with HDsz is best expressed on the flanks of the Frøya High central salient, whereas the intrabasement seismic signature within the salient itself shows a significant convex upwards geometry (Figure 3). This could either represent a folding of the Ksz, or an upwarping of the seismic facies signature associated with the HDsz. As reported by e.g., Wiest et al. (2020) and Fazlikhani et al. (2017) from the Bergen Arc region and the northern North Sea, respectively, shear zones are typically observed as several bands of mylonitic fabrics. Figure 3b shows how parts of the Ksz fabric is preserved even within the degraded footwall, merging with an upwarped stringer of what we interpret as the HDsz. This observation suggests backrotation and uplift of the Frøya High during the growth of the KFC.

5.2 The Frøya High Turtleback

The KFC enveloping the degraded Frøya High has previously been interpreted as a result of lateral linkage of faults producing a zig-zag fault pattern (Muñoz-Barrera et al., 2020). This model is consistent with that of Fossen and Rotevatn (2016) for sinusoidal geometries of the faults surrounding the Salt Lake and Gullfaks salients in Utah, USA, and the Norwegian North Sea, respectively. The salients are 40-50 km wide, comparable in size to the 45 km wide central salient of the Frøya High. However, the systems differ in displacements by a tenfold, as measurable displacements along the KFC ranges between 20 - 40 km, whilst displacements surrounding e.g., the Gullfaks field are in the order of 2-4 km (Fossen & Rotevatn, 2016). The associated footwall uplift in these systems can therefore be expected to have significantly different magnitudes, and strongly varying resultant geometries. Lateral fault-linkage typically entails producing a relay structure between the fault tips during fault linkage and a corresponding synclinal depression in the footwall after reaching the through-going fault-linkage evolutionary stage (Fossen & Rotevatn, 2016; Gawthorpe & Leeder, 2000) (Figure 7a). The hangingwall response to this process entails two synclinal depocenters juxtaposing the area of linkage, corresponding to areas of maximum displacement in the original fault segments (Figure 7a). The Frøya High has two synclinal depocenters flanking the central salient of the high (Figure 2 and 8a), much like described in the fault linkage model. However, the central salient exhibits a radial pattern of incising valleys (Figures 2 and 8a), indicating that the highest footwall topography prior to the latest event of erosion was located on the salient itself, and not in the area of maximum displacement of the individual fault's segments. The latter scenario would produce erosional features on the flanks of the current salient, and the area of linkage would propose the largest drainage system from footwall to hangingwall (Figure 7a) (Gawthorpe & Leeder, 2000). Also, producing a salient in the area of fault linkage would require symmetrical faults developing simultaneously and with little to no spatial difference along the strike of the system. We therefore deem it unlikely that the current configuration of the Frøya High is a result of fault-linkage between separate faults north and south of the current central salient. Rather, the current configuration of the Frøya High (Figure 8a) is consistent with the endmember for the model entailing a detachment fault system where displacement and deformation localizes along one major fault segment during development, followed by significant erosion (Figure 7b).

In extensional tectonic environments, radial patterns of incising valleys as observed on the Frøya High are typically seen onshore in core complex scenarios, a contemporarily well exposed analogue being the Copper Canyon Turtleback in the Basin and Range Province, western US (Figure 8). Two main schools of thought exist when addressing turtleback structure formation in continental settings; that of localized isostatic uplift due to a rolling hinge model scenario developing in the area of maximum displacement (Brun et al., 2018; Gresseth et al., 2022; Kapp et al., 2008), and that of orthogonal shortening in a transtensional strain field (Dewey, 2002; Krabbendam & Dewey, 1998; Vetti & Fossen, 2012). Recent works from the WGR onshore Norway also show how major extension-parallel anticlines in the footwall may be a result of footwall uplift and orthogonal shortening, with amplifying effects and pronounced effects on associated basin architectures (Osmundsen et al., 2022). In the Basin and Range province, a dextral transtensional system which effectively folded the detachment fault plane is invoked to explain turtleback structures with a mylonitic carapace (Dewey, 2002; Holm et al., 1994).

A relationship between the exhumation of the Death Valley Turtlebacks and the mechanisms of isostatic uplift and has not yet been suggested. The lack of exploring this possibility may be scale dependent. Unlike the c. 3,5 km wide Copper Canyon turtleback, the Frøya turtleback is approximately 45 km wide, and constitutes the footwall where the KFC effectively thins the crust from 26 km to 11 km, with displacements ranging from 20 to 40 km (Muñoz-Barrera et al., 2020). Notably, these numbers may be significantly higher as in large-scale fault systems, flexural rotation of the footwall in large-scale fault systems may lead to a flattening upwards fault, giving the slip surface a convex-up geometry. Down-dip continuation of such detachment faults may remain active for a long time and continue to accommodate substantial amounts of extension and consequently lead to continued footwall exhumation. Eventually, the slip surface may form the top basement surface over considerable distances (Lavier & Manatschal, 2006; Lavier et al., 1999; Reston, 2009). The exhumation may simultaneously lead to footwall and detachment shear zone erosion, adding uncertainty with respect to the quantification of crustal thinning (Osmundsen & Péron-Pinvidic, 2018). According to Reston (2009) and McDermott and Reston (2015), the flexural high of an exhumed footwall may be interpreted as a second fault scarp in seismic data, leading to an extension discrepancy. Following this argumentation, the peneplained footwall of the Frøya High (e.g., Figure 8a) indicate that the measurable displacement along the KFC is underestimated. Potential field anomaly data (Figure 6 and (Muñoz-Barrera et al., 2020)) indicate that the footwall consists of exhumed mid to lower crustal rocks. As such, a comparison between the Frøya Turtleback and the Copper Canyon turtlebacks may provide insights and context to the erosion mechanisms and thus paleo-topography, but not necessarily the mechanisms causing the resultant geometry of the footwall uplift. Analogue and numerical modeling, however, provides insights into extensional processes that may produce the turtleback structures in strain regimes not affected by transtension.

Wernicke (1995) challenged the principles of Andersonian fault theory, which predicted that normal faults with dip angles < 30° could not slip (Anderson, 1905). Wernicke (1995) (see also (Buck, 1988; Hamilton, 1988; Lister & Davis, 1989; Wernicke & Axen, 1988)) introduced the rolling hinge model, suggesting that isostatic unloading during and after slip effectively tilts and induces short-wavelength flexure of the footwall in systems involving kilometer-scale displacements. Lavier et al. (1999) used numerical modeling to investigate footwall configuration in detachment faults accommodating tens of kilometers of displacement and show in 2D how the area of maximum displacement corresponds to that of a rolling hinge with a backrotated, subhorizontal detachment after 27 km of displacement. Figure 4 of Brun et al. (2018) shows how the resultant core complex exhumation may localize in and that local exhumation and upwelling of ductile crust may lead to sinusoidal detachment faults. Few of the mentioned models include the along-strike structural morphology and its consequences during and after development of the local footwall uplift and sinusoidal detachment fault plane geometry. Figure 7b illustrates the principles as outlined above in 3D.

Non-linearity in the slip direction generates space problems leading to hanging- or footwall strain (Fossen, 2016, p. 179). This entails that during the evolution of a detachment fault which gradually attains an increasing sinusoidal geometry the effective strain will vary along-strike of the fault segment, also during a constant stress field (Figure 9). On the Frøya High, the flanks of the interpreted turtleback structure show varying geometries to the north and south. In the northern structural recess, a Jurassic basin resides at high crustal levels constrained from the Rås Basin by a younger fault splay than the original KFC detachment fault surface (Figure 4). Similar scenarios can be observed in literature concerning reactivation of sinusoidal detachment fault systems elsewhere; Miller and Pavlis (2005: Figure 7); Knott et al. (2005: Figure 8); Kapp et al. (2008: Figure 4); Brun et al. (2018: Figure 4). Albeit, the relationship between original detachment fault planes and younger faults originating at a higher angle to the direction of extension has until now not been addressed. We suggest that increasing sinuosity of the KFC during the exhumation of the Frøya High Turtleback would eventually require the slip on the flanks of the turtleback to evolve from dip-slip during early-stage development, to an oblique-slip and even strike-slip during continued displacement (Figure 9). The younger fault splay of the KFC in the northern structural recess likely represents successive incision and lateral linkage as a response to the varying strain affecting the original detachment fault plane during pulses of detachment reactivation (Figures 4 and 9).

The same geometries cannot be recognized in the southern structural recess, where the KFC incises into the ENE-SSW oriented Slørebotn detachment. However, this area remains is highly influenced by the MTFC-trend also during Mesozoic rifting (e.g., Bunkholt et al., 2021; Muñoz-Barrera et al., 2022). During the Late Jurassic, the Slørebotn Subbasin shows major (up to 60°) fault block rotation (Jongepier et al., 1996), possibly accommodating for the increasingly complex strain field development during this rift stage. Based on the argumentation as outlined above, we find it likely that multiple faults develop and incise the crust during the necking phase, and that local events of successive incisions may occur also within detachment fault systems during rift margin development. The central salient and northern structural recess provides evidence for several processes in one place: localized isostatic uplift in the turtleback structure, successive incision forming the youngest fault splay, and lateral linkage of elder and younger fault segment within the KFC. Effectively, this outlines the KFC as a diachronous fault complex, consisting of fault segments generated at various stages through time.

5.3 Potential field data correlation

The gravity anomaly distribution within the study coincides with the mapped top metamorphic basement and thus the extent of the Frøya High (Figures 2 and 6a). The magnetic anomaly response, however, has previously been interpreted to represent magnetic salients within the high, the highest values east of the northern structural recess to represent a metamorphic core complex (Muñoz-Barrera et al., 2020). We argue however, based on the interpretation of the Frøya Highs development in terms of a rolling hinge model effectively producing a turtleback structure, that the highest anomaly value represents the top of the offshore continuation of the Høybakken detachment. As shown in Figure 3, the Ksz exploits the HD shear zone template to a varying degree along-strike, with cross-cutting and overprinting relationships within the central salient, while reactivating it to a lesser degree in the northern structural recess. East of the southern structural recess, the magnetic anomaly response in the area of the Slørebotn Subbasin and the Gossa High is lower relative to those recorded east of the northern structural recess. The latter area represents a tectonic scenario where the Høybakken Detachment is reactivated and incised by the KFC (Figure 3c) (Muñoz-Barrera et al., 2020; Osmundsen & Péron-Pinvidic, 2018). The same scenario is interpreted for the central salient based on intrabasement seismic reflection patterns (Figure 3b), whilst the northern structural recess represents an area of less exploitation of the Høybakken Detachment shear fabrics, and rather a further development and larger magnitude of the Ksz (Figure 3a). We argue that the magnetic anomalies within the study area largely represent the geometry of the offshore continuation of the HD but show lower anomalies where the HD is largely incised and overprinted by Mesozoic events, as for the Slørebotn detachment and in the central part of the Frøya High. The high magnetic anomaly in the Froan basin east of the large culmination within the Frøya High corresponds to the upwarped "scoop shaped detachment fault" described in Osmundsen et al. (2021). In summary, and in line with previous publications, the magnetic anomaly response on the Norwegian continental shelf is strongly variable and do not necessarily correspond to maximum footwall exhumation during Mesozoic rift events (Osmundsen & Ebbing, 2008). The magnetic anomaly response in the study area may very well reflect detachment geometries and lithological heterogeneities inherited from Devonian transtension or, alternatively, from Late Paleozoic/Early Mesozoic structures that modified the Devonian structural template.

5.4 Footwall erosional surfaces separated by knick-points: evidence for a rotating footwall

Across the Frøya High, we have mapped a series of knick-points that, when connected, combine into fault transverse ridges that effectively separate differently dipping segments of the detachment footwall (Figure 5). Lymer et al. (2022) postulated that knick-points observed on a detachment surface in the Porcupine basin, west of Ireland correspond to former locations where new fault families soled out onto the detachment as the detachment rotated backward with increasing extension. This would be consistent with the rolling hinge model *sensu* Lavier et al. (1999) and Brun et al. (2018). However, on the Frøya High, the differently dipping segments correspond to zones which indicate their own specific chrono- and lithostratigraphy above the top of basement indicating that the different dipping top basement segments correspond to unconformities and are related to discrete events of erosion. Based on seismic-to-well-ties in 6306/10-1, 6306/6-1, 6306/6-2, and 6407/10-3, the respective top basement segments are correlated to the IMU, BCU and BCenU regional unconformities. They also erode and partly incise each other in specific zones across the high. We note that the surfaces are mapped in seismic data in the time domain, and their geometries might be affected by depth conversion. However, despite a possible change in angle, the knick-point geometry will remain as they do not correspond to variations in the overlying sedimentary facies and thus not significant variations in overburden velocities. The differential dip between the surfaces is a likely result of multiple erosional events occurring during continued footwall topographic uplift associated with the rolling hinge model. The youngest erosional surfaces thus hold the potential for partly or fully obliterating the remnants of older drainage systems. Points of fault linkage may have been present at certain points, but our model entails that such linkage traces are presently removed by erosion.

5.5 Rås Basin supradetachment basin configuration

In published literature, categorizing a sedimentary basin as a supradetachment basin typically requires the basin to reside in the hangingwall of low-angle (<30°), high-displacement (>5 km) normal faults, juxtaposed rocks exhumed from middle to lower crustal levels due to extension (e.g., Friedmann & Burbank, 1995; Lister et al., 1984b; Whitney et al., 2013). Despite increasing interest in recent years, the source-to-sink relationships in supradetachment basins remain poorly understood compared to traditional rift basins recording less extension (e.g., Gawthorpe et al., 1994; Henstra et al., 2017). Onshore studies of supradetachment basins rely on analysis of sedimentary and stratigraphic relationships (e.g., Serck et al., 2021; Steel et al., 1977). The megasequences observed in seismic data in the Rås Basin remain inaccessible and undrilled due to their current depths. However, the megasequences may be tentatively dated based on correlation between their seismic facies' signatures and the erosional history and dated unconformities up-dip on the Frøya High. As such, a pre-Cretaceous syntectonic supradetachment basin present in the Rås Basin (Figures 3 and 8). The spoon-shaped supradetachment basin in the southern structural recess is bound by the KFC and the Main Møre boundary fault, holds three megasequences and records deposition during two rift episodes during inferred late Middle to Late Jurassic and earliest Cretaceous times (Figure 3 and Muñoz-Barrera et al. (2022)). Figures 3 and 8a shows how the supradetachment basin flanks the central salient and that pre-Cretaceous deposits are present also in the northern structural recess. The sedimentary thickness in the northern structural recess largely coincides with that recorded in the southern structural recess (Figure 3). However, geometrical differences may be observed in the distribution of the strata (Figure 3d). The undulating seismic facies signatures observed in the southern structural recess strongly contrasts with the more tabular to wedge-shaped distribution in the northern structural recess (Figure 3d). Lack of 3D data and sufficiently tightly spaced 2D seismic lines in this study area hampers a well-constrained explanation for the geometrical differences, as they may also be results of observing similar sedimentary strata at slightly different angles to the direction of sediment distribution.

A notable, and more robust observation from the proposed source area is the nature of the radial pattern of incising valleys dispersed from the central salient of the Frøya High, clearly indicating sedimentary input into both synclinal depocenters associated with the structural recesses. This indicates that one can deduce a similar source-to-sink mechanism from the Frøya High into the Rås basin for both the southern and northern structural recesses. A notable difference is the perched Jurassic basin in the hangingwall in the northern structural recess (Figures 3a and 4). Well 6306/5-2 drilled sandstone deposits of Middle to early Late Jurassic age in this rider block hanging wall basin (NPD, 2022) (Figure 4). In seismic data, the corresponding seismic horizon shows incising valleys, indicating a cannibalization of these deposits during sediment distribution into the northern structural recess basin during earliest Cretaceous. This insinuates the presence of both eroded basement and reworked Jurassic hangingwall basin deposits in the northern structural recess basin. Similarly, the southern structural recess could have received sedimentary infill sourced from the eroded fault-blocks in the Slørebotn subbasin and the associated Jurassic sedimentary fill in these basins (Jongepier et al., 1996) (Figure 3c), but this remains unconstrained.

6 Conclusions

For this study, we have incorporated 2D and 3D seismic reflection, potential field and well data to investigate the 3D evolution of the necking domain in the southern mid-Norwegian Rifted margin. The structural configuration of the study area has been compared to suspected onshore analogues, and to published numerical and analogue modelling results. Our interpretations honor and incorporate previous studies of the mid-Norwegian margin, and we conclude the following:

- Growth of large-scale detachment faults in necking domains are associated with displacements of several tens of kilometers and involve middle to lower crustal material. The pattern of exhumation of the associated basement fabrics affects detachment fault geometry.
- Detachment fault systems experience increasing lateral sinuosity where footwall exhumation localizes in the area of maximum displacement. This will in turn lead to

elevation of local topography in the footwall and increased sensitivity to base-level drop in central parts of the detachment fault segment during evolution. Correspondingly, geometrical adjustments of the detachment fault plane during displacement will affect and control depocenter distribution in the hangingwall throughout the active phase of the system. Consequently, associated sedimentary dispersal patterns will be continuously modified and prone to sediment rerouting and cannibalization.

- Where obtaining sinusoidal fault geometries, detachment faults will locally experience increased shear stresses in areas flanking the area of maximum displacement if displacement continues under a close to constant strain field. This motivates successive incision and lateral linkage, producing detachment fault systems with segments generated at various stages of the system evolution.
- The structural configuration of the Frøya High on the mid-Norwegian margin was mainly controlled by the large-magnitude Klakk Fault Complex, which functioned as a combined inner and outer necking breakaway complex where constraining the Frøya High from the Rås Basin. Central parts of the Frøya High represent an eroded turtleback structure, established during increasing crustal thinning and increasing sinuosity development along the Klakk Fault Complex during Middle Jurassic to Early Cretaceous rifting.
- The antidomal exhumation pattern of the footwall turtleback structure set up a radial dispersal pattern of incising valleys and pathways for sediment transport from the Frøya High central salient in the footwall to the Rås Basin in its hangingwall. Detachment fault evolution led to establishment of synclinal depocenters to the north and south of the central salient. The sedimentary strata are correlatable along-strike, linking the main basin segments into a major supradetachment basin.
- The fault-parallel ridges on the Frøya High, separating the top basement surface into three distinct footwall segments with varying dips reveal that significant erosion affected the high during discrete periods following footwall uplift. The varying dips of the eroded top basement provide evidence for severe back rotation during footwall uplift, consistent with the rolling hinge model.

Acknowledgements

This contribution forms part of the Suprabasins Project funded by the Research Council of Norway (project number: 295208) under the call: PETROMAKS 2 – Large-scale Programme for Petroleum Research, and by the following industry partners: Aker BP ASA, Spirit Energy Norge AS, Equinor ASA and Lundin Norway. Public data used in this contribution are stored in the Norwegian Petroleum Directorate DISKOS database. We thank Schlumberger for supporting the Norwegian University of Science and Technology with the academic license for the Petrel 2020 software (https://www.software.slb.com/products/petrel) and find ourselves indebted to members of the Suprabasins community for fruitful and inspiring discussions throughout the project. The content of this article remains, however, the sole responsibility of the authors.

Data Availability Statement

All seismic data used to produce interpreted maps and cross-sections presented in this study are public and can be requested through the DISKOS database administrated by the Norwegian Petroleum Directorate. Version 2020.4 of the Petrel E&P Software Platform used for seismic interpretation is available via appropriate licensing via Schlumberger Limited: https://www.software.slb.com/products/petrel. Potential field data maps as displayed in Figure 6 are available in Olesen et al. (2010a) and Olesen et al. (2010b).

References

Andersen, T. B., & Jamtveit, B. (1990). Uplift of deep crust during orogenic extensional collapse: A model based on field studies in the Sogn-Sunnfjord region of western Norway. *Tectonics, 9*(5), 1097-1111.

Anderson, E. M. (1905). The dynamics of faulting. *Transactions of the Edinburgh Geological Society, 8*(3), 387-402. doi:doi:10.1144/transed.8.3.387

Bell, R. E., Jackson, C. A.-L., Elliott, G. M., Gawthorpe, R. L., Sharp, I. R., & Michelsen, L. (2014). Insights into the development of major rift-related unconformities from geologically constrained subsidence modelling: Halten Terrace, offshore mid Norway. *Basin Research, 26*(1), 203-224. doi:https://doi.org/10.1111/bre.12049

Blaich, O. A., Faleide, J. I., & Tsikalas, F. (2011). Crustal breakup and continent-ocean transition at South Atlantic conjugate margins. *Journal of Geophysical Research: Solid Earth, 116*(B1).

Blystad, P., Brekke, H., Færseth, R. B., Larsen, B. T., Skogseid, J., & Tørudbakken, B. (1995). Structural elements of the Norwegian continental shelf. Part 2: The Norwegian Sea region. *NPD Bull., 8*.

Brun, J.-P., Sokoutis, D., Tirel, C., Gueydan, F., Van Den Driessche, J., & Beslier, M.-O. (2018). Crustal versus mantle core complexes. *Tectonophysics, 746*, 22-45. doi:https://doi.org/10.1016/j.tecto.2017.09.017

Braathen, A., Nordgulen, O., Osmundsen, P. T., Andersen, T. B., Solli, A., & Roberts, D. (2000). Devonian, orogen-parallel, opposed extension in the Central Norwegian Caledonides. *Geology, 28*(7), 615-618. doi:10.1130/0091-7613(2000)28<615:DOOEIT>2.0.CO;2

Braathen, A., Osmundsen, P. T., & Gabrielsen, R. H. (2004). Dynamic development of fault rocks in a crustal-scale detachment: An example from western Norway. *Tectonics, 23*(4).

Braathen, A., Osmundsen, P. T., Nordgulen, Ø., Roberts, D., & Meyer, G. B. (2002). Orogen-parallel extension of the Caledonides in northern Central Norway: an overview. *Norwegian Journal of Geology/Norsk Geologisk Forening, 82*(4).

Buck, W. R. (1988). Flexural rotation of normal faults. *Tectonics, 7*(5), 959-973. doi:https://doi.org/10.1029/TC007i005p00959

Bunkholt, H., Oftedal, B., Hansen, J., Løseth, H., & Kløvjan, O. (2021). Trøndelag Platform and Halten–Dønna Terraces Composite Tectono-Sedimentary Element, Norwegian Rifted Margin, Norwegian Sea. *Geological Society, London, Memoirs*, M57-2017. doi:10.1144/M57-2017-13

Chenin, P., Manatschal, G., Picazo, S., Müntener, O., Karner, G., Johnson, C., & Ulrich, M. (2017). Influence of the architecture of magma-poor hyperextended rifted margins on orogens produced by the closure of narrow versus wide oceans. *Geosphere, 13*(2), 559-576.

Corfu, F., Andersen, T., & Gasser, D. (2014). The Scandinavian Caledonides: main features, conceptual advances and critical questions. *Geological Society, London, Special Publications, 390*(1), 9-43.

Dewey, J. F. (2002). Transtension in Arcs and Orogens. *International Geology Review, 44*(5), 402-439. doi:10.2747/0020-6814.44.5.402

Doré, A. G., Lundin, E. R., Fichler, C., & Olesen, O. (1997). Patterns of basement structure and reactivation along the NE Atlantic margin. *Journal of the Geological Society, 154*(1), 85-92. doi:10.1144/gsjgs.154.1.0085

Doré, A. G., Lundin, E. R., Jensen, L. N., Birkeland, Ø., Eliassen, P. E., & Fichler, C. (1999). *Principal tectonic events in the evolution of the northwest European Atlantic margin.* Paper presented at the Geological society, London, petroleum geology conference series.

Dunlap, W., & Fossen, H. (1998). Early Paleozoic orogenic collapse, tectonic stability, and late Paleozoic continental rifting revealed through thermochronology of K-feldspars, southern Norway. *Tectonics, 17*(4), 604-620.

Escartín, J., Mével, C., Petersen, S., Bonnemains, D., Cannat, M., Andreani, M., . . . Garcia, R. (2017). Tectonic structure, evolution, and the nature of oceanic core complexes and their detachment fault zones (13°20′N and 13°30′N, Mid Atlantic Ridge). *Geochemistry, Geophysics, Geosystems, 18*(4), 1451-1482. doi:https://doi.org/10.1002/2016GC006775

Faleide, J. I., Tsikalas, F., Breivik, A., Mjelde, R., Ritzmann, O., Engen, O., . . . Eldholm, O. (2008). Structure and evolution of the continental margin off Norway and the Barents Sea. *Episodes, 31*, 82-91. doi:10.18814/epiiugs/2008/v31i1/012

Fazlikhani, H., Fossen, H., Gawthorpe, R. L., Faleide, J. I., & Bell, R. E. (2017). Basement structure and its influence on the structural configuration of the northern North Sea rift. *Tectonics, 36*(6), 1151-1177.

Fossen, H. (2010). Extensional tectonics in the North Atlantic Caledonides: a regional view. *Geological Society, London, Special Publications, 335*(1), 767-793.

Fossen, H. (2016). *Structural Geology* (2 ed.). Cambridge: Cambridge University Press.

Fossen, H., & Rotevatn, A. (2016). Fault linkage and relay structures in extensional settings—A review. *Earth-Science Reviews, 154*, 14-28. doi:https://doi.org/10.1016/j.earscirev.2015.11.014

Friedmann, S. J., & Burbank, D. W. (1995). Rift basins and supradetachment basins: Intracontinental extensional end-members. *Basin Research, 7*(2), 109-127.

Gabrielsen, R., Braathen, A., Dehls, J., & Roberts, D. (2002). Tectonic lineaments of Norway. *Norwegian Journal of Geology, 82*, 153-174.

Gabrielsen, R. H., Odinsen, T., & Grunnaleite, I. (1999). Structuring of the Northern Viking Graben and the Møre Basin; the influence of basement structural grain, and the particular role of the Møre-Trøndelag Fault Complex. *Marine and Petroleum Geology, 16*, 443-465.

Gawthorpe, R. L., Fraser, A. J., & Collier, R. E. L. (1994). Sequence stratigraphy in active extensional basins: implications for the interpretation of ancient basin-fills. *Marine and Petroleum Geology, 11*(6), 642-658.

Gawthorpe, R. L., & Leeder, M. R. (2000). Tectono-sedimentary evolution of active extensional basins. *Basin Research, 12*(3-4), 195-218. doi:https://doi.org/10.1111/j.1365-2117.2000.00121.x

Gee, D. G., Janák, M., Majka, J., Robinson, P., & van Roermund, H. (2013). Subduction along and within the Baltoscandian margin during closing of the Iapetus Ocean and Baltica-Laurentia collision. *Lithosphere, 5*(2), 169-178.

Google. (2022). Google Earth Pro. Available from https://www.google.com/earth/versions/#earth-pro

Gouiza, M., & Naliboff, J. (2021). Rheological inheritance controls the formation of segmented rifted margins in cratonic lithosphere. *Nature Communications, 12*(1), 4653. doi:10.1038/s41467-021-24945-5

Gresseth, J. L. S., Braathen, A., Serck, C. S., Faleide, J. I., & Osmundsen, P. T. (2022). Late Paleozoic supradetachment basin configuration in the southwestern Barents Sea—Intrabasement seismic facies of the Fingerdjupet Subbasin. *Basin Research, 34*(2), 570-589. doi:https://doi.org/10.1111/bre.12631

Grønlie, A., & Roberts, D. (1989). Resurgent strike-slip duplex development along the Hitra-Snåsa and Verran Faults, Møre-trøndelag fault zone, Central Norway. *Journal of Structural Geology, 11*(3), 295-305. doi:https://doi.org/10.1016/0191-8141(89)90069-2

Hamilton, W. B. (1988). Detachment faulting in the Death Valley region, California and Nevada. *U. S. Geological Survey Bulletin, 1790*, 51-85.

Henstra, G. A., Gawthorpe, R. L., Helland-Hansen, W., Ravnås, R., & Rotevatn, A. (2017). Depositional systems in multiphase rifts: seismic case study from the Lofoten margin, Norway. *Basin Research, 29*(4), 447-469.

Holm, D. K., Fleck, R. J., & Lux, D. R. (1994). The Death Valley Turtlebacks Reinterpreted as Miocene-Pliocene Folds of a Major Detachment Surface. *The Journal of Geology, 102*(6), 718-727. doi:10.1086/629715

Jolivet, L., Faccenna, C., Huet, B., Labrousse, L., Le Pourhiet, L., Lacombe, O., . . . Driussi, O. (2013). Aegean tectonics: Strain localisation, slab tearing and trench retreat. *Tectonophysics, 597-598*, 1-33. doi:https://doi.org/10.1016/j.tecto.2012.06.011

Jongepier, K., Rui, J. C., & Grue, K. (1996). Triassic to Early Cretaceous stratigraphic and structural development of the northeastern Møre Basin margin, off Mid-Norway. *Norwegian Journal of Geology, 76*(4), 199-214.

Kapp, P., Taylor, M., Stockli, D., & Ding, L. (2008). Development of active low-angle normal fault systems during orogenic collapse: Insight from Tibet. *Geology, 36*(1), 7-10.

Knott, J. R., Sarna-Wojcicki, A. M., Machette, M. N., & Klinger, R. E. (2005). Upper Neogene stratigraphy and tectonics of Death Valley — a review. *Earth-Science Reviews, 73*(1), 245-270. doi:https://doi.org/10.1016/j.earscirev.2005.07.004

Krabbendam, M., & Dewey, J. F. (1998). Exhumation of UHP rocks by transtension in the Western Gneiss Region, Scandinavian Caledonides. *Geological Society, London, Special Publications, 135*(1), 159-181.

Lavier, L. L., & Manatschal, G. (2006). A mechanism to thin the continental lithosphere at magma-poor margins. *Nature, 440*(7082), 324-328. doi:10.1038/nature04608

Lavier, L. L., Roger Buck, W., & Poliakov, A. N. B. (1999). Self-consistent rolling-hinge model for the evolution of large-offset low-angle normal faults. *Geology, 27*(12), 1127-1130. doi:10.1130/0091-7613(1999)027<1127:Scrhmf>2.3.Co;2

Lenhart, A., Jackson, C. A.-L., Bell, R. E., Duffy, O. B., Gawthorpe, R. L., & Fossen, H. (2019). Structural architecture and composition of crystalline basement offshore west Norway. *Lithosphere, 11*(2), 273-293.

Lien, T. (2005). From rifting to drifting: effects on the development of deep-water hydrocarbon reservoirs in a passive margin setting, Norwegian Sea. *Norwegian Journal of Geology/Norsk Geologisk Forening, 85*(4).

Lister, G. S., Banga, G., & Feenstra, A. (1984a). Metamorphic core complexes of Cordilleran type in the Cyclades, Aegean Sea, Greece. *Geology, 12*(4), 221-225. doi:10.1130/0091-7613(1984)12<221:Mccoct>2.0.Co;2

Lister, G. S., & Davis, G. A. (1989). The origin of metamorphic core complexes and detachment faults formed during Tertiary continental extension in the northern Colorado River region, U.S.A. *Journal of Structural Geology, 11*(1), 65-94. doi:https://doi.org/10.1016/0191-8141(89)90036-9

Lister, G. S., Davis, G. A., McClelland, W. C., & Marcott, D. T. (1984b). Complexities in the evolution of low-angle crustal shear zones during continental extension. *The Geological Society of America, 97th annual meeting, 16*(6), 577.

Lymer, G., Childs, C., & Walsh, J. (2022). *Punctuated propagation of a corrugated extensional detachment offshore West of Ireland*. Retrieved from

Lymer, G., Cresswell, D. J., Reston, T. J., Bull, J. M., Sawyer, D. S., Morgan, J. K., . . . Shillington, D. J. (2019). 3D development of detachment faulting during continental breakup. *Earth and Planetary Science Letters, 515*, 90-99.

Manatschal, G. (2004). New models for evolution of magma-poor rifted margins based on a review of data and concepts from West Iberia and the Alps. *International Journal of Earth Sciences, 93*(3), 432-466.

McDermott, K., & Reston, T. (2015). To see, or not to see? Rifted margin extension. *Geology, 43*(11), 967-970. doi:10.1130/g36982.1

Miller, M. B., & Pavlis, T. L. (2005). The Black Mountains turtlebacks: Rosetta stones of Death Valley tectonics. *Earth-Science Reviews, 73*(1), 115-138. doi:https://doi.org/10.1016/j.earscirev.2005.04.007

Mohn, G., Karner, G. D., Manatschal, G., & Johnson, C. A. (2015). Structural and stratigraphic evolution of the Iberia–Newfoundland hyper-extended rifted margin: a quantitative modelling approach. *Geological Society, London, Special Publications, 413*(1), 53-89.

Mohn, G., Manatschal, G., Beltrando, M., Masini, E., & Kusznir, N. (2012). Necking of continental crust in magma-poor rifted margins: Evidence from the fossil Alpine Tethys margins. *Tectonics, 31*(1). doi:https://doi.org/10.1029/2011TC002961

Mortimer, E. J., Gouiza, M., Paton, D. A., Stanca, R., Rodriguez, K., Hodgson, N., & Hussein, A. A. (2020). Architecture of a magma poor passive margin – Insights from the Somali margin. *Marine Geology, 428*, 106269. doi:https://doi.org/10.1016/j.margeo.2020.106269

Muñoz-Barrera, J. M., Rotevatn, A., Gawthorpe, R. L., Henstra, G., & Kristensen, T. B. (2022). Supradetachment basins in necking domains of rifted margins: Insights from the Norwegian Sea. *Basin Research, 34*(3), 991-1019. doi:https://doi.org/10.1111/bre.12648

Muñoz-Barrera, J. M., Rotevatn, A., Gawthorpe, R. L., Henstra, G. A., & Kristensen, T. B. (2020). The role of structural inheritance in the development of high-displacement crustal faults in the necking domain of rifted margins: The Klakk Fault Complex, Frøya High, offshore mid-Norway. *Journal of Structural Geology, 140*, 104163.

Nonn, C., Leroy, S., Khanbari, K., & Abdulhakim, A. (2017). Tectono-sedimentary evolution of the eastern Gulf of Aden conjugate passive margins: Narrowness and asymmetry in oblique rifting context. *Tectonophysics, 721*. doi:10.1016/j.tecto.2017.09.024

Norton, M. G. (1986). Late Caledonide Extension in western Norway: A response to extreme crustal thickening. *Tectonics, 5*, 195-204.

NPD. (2022). Norwegian Petroleum Directorate Factpages. Available from https://factpages.npd.no/

Olesen, O., Ebbing, J., Gellein, J., Kihle, O., Myklebust, R., Sand, M., . . . Solheim, D. (Cartographer). (2010a). Gravity anomaly map, Norway and adjacent areas. Retrieved from https://www.ngu.no/en/publikasjon/gravity-anomaly-map-norway-and-adjacent-areas-scale-13-mill

Olesen, O., Gellein, J., Gernigon, L., Kihle, O., Koziel, J., Lauritsen, T., . . . Skilbrei, J. R. (Cartographer). (2010b). Magnetic anomaly map, Norway and adjacent areas. Retrieved from https://www.ngu.no/en/publikasjon/magnetic-anomaly-map-norway-and-adjacent-areas-scale-13-mill

Osmundsen, P., & Andersen, T. (2001). The middle Devonian basins of western Norway: sedimentary response to large-scale transtensional tectonics? *Tectonophysics, 332*(1-2), 51-68.

Osmundsen, P., Braathen, A., Nordgulen, Ø., Roberts, D., Meyer, G., & Eide, E. (2003). The Devonian Nesna shear zone and adjacent gneiss-cored culminations, North–Central Norwegian Caledonides. *Journal of the Geological Society, 160*(1), 137-150.

Osmundsen, P. T., & Ebbing, J. (2008). Styles of extension offshore mid-Norway and implications for mechanisms of crustal thinning at passive margins. *Tectonics, 27*(6). doi:https://doi.org/10.1029/2007TC002242

Osmundsen, P. T., Eide, E., Haabesland, N., Roberts, D., Andersen, T., Kendrick, M., . . . Redfield, T. (2006). Kinematics of the Høybakken detachment zone and the Møre–Trøndelag Fault Complex, central Norway. *Journal of the Geological Society, 163*(2), 303-318.

Osmundsen, P. T., & Péron-Pinvidic, G. (2018). Crustal-scale fault interaction at rifted margins and the formation of domain-bounding breakaway complexes: Insights from offshore Norway. *Tectonics, 37*(3), 935-964.

Osmundsen, P. T., Péron-Pinvidic, G., Gresseth, J. L. S., & Braathen, A. (2022). *3D evolution of extensional detachment faults and their effect on the architecture of rifts and rifted margins*. Paper presented at the EGU General Assembly 2022, Vienna, Austria.

Osmundsen, P. T., & Péron-Pinvidic, G. (2018). Crustal-scale fault interaction at rifted margins and the formation of domain-bounding breakaway complexes: Insights from offshore Norway. *Tectonics, 37*(3), 935-964.

Osmundsen, P. T., Péron-Pinvidic, G., & Bunkholt, H. (2021). Rifting of collapsed orogens: successive incision of continental crust in the proximal margin offshore Norway. *Tectonics, 40*(2), e2020TC006283.

Osmundsen, P. T., & Redfield, T. (2011). Crustal taper and topography at passive continental margins. *Terra Nova, 23*(6), 349-361.

Osmundsen, P. T., Sommaruga, A., Skilbrei, J. R., & Olesen, O. (2002). Deep structure of the Mid Norway rifted margin. *Norwegian Journal of Geology/Norsk Geologisk Forening, 82*(4).

Péron-Pinvidic, G., Fourel, L., & Buiter, S. J. H. (2022a). The influence of orogenic collision inheritance on rifted margin architecture: Insights from comparing numerical experiments to the Mid-Norwegian margin. *Tectonophysics, 828*, 229273. doi:https://doi.org/10.1016/j.tecto.2022.229273

Péron-Pinvidic, G., & Manatschal, G. (2009). The final rifting evolution at deep magma-poor passive margins from Iberia-Newfoundland: a new point of view. *International Journal of Earth Sciences, 98*(7), 1581-1597.

Péron-Pinvidic, G., Manatschal, G., & Osmundsen, P. T. (2013). Structural comparison of archetypal Atlantic rifted margins: A review of observations and concepts. *Marine and Petroleum Geology, 43*, 21-47. doi:10.1016/j.marpetgeo.2013.02.002

Peron-Pinvidic, G., Manatschal, G., & Participants, I. R. W. (2019). Rifted margins: State of the art and future challenges. *Frontiers in Earth Science, 7*, 218.

Peron-Pinvidic, G., Osmundsen, P., & Bunkholt, H. (2020). The proximal domain of the Mid-Norwegian rifted margin: the Trøndelag Platform revisited. *Tectonophysics, 790*, 228551.

Péron-Pinvidic, G., Åkermoen, T., & Leivestad, L. I. (2022b). The North-East Atlantic Mid-Norwegian rifted margin: Insights from the deep imaging Geoex MCG RDI19 dataset. *Tectonophysics, 824*, 229225.

Phillips, T., Jackson, C., Bell, R., Duffy, O., & Fossen, H. (2016). Reactivation of intrabasement structures during rifting: A case study from offshore southern Norway. *Journal of Structural Geology, 91*. doi:10.1016/j.jsg.2016.08.008

Redfield, T., Braathen, A., Gabrielsen, R., Osmundsen, P., Torsvik, T., & Andriessen, P. (2005). Late Mesozoic to early Cenozoic components of vertical separation across the Møre–Trøndelag Fault Complex, Norway. *Tectonophysics, 395*(3-4), 233-249.

Redfield, T. F., Torsvik, T. H., Andriessen, P. A. M., & Gabrielsen, R. H. (2004). Mesozoic and Cenozoic tectonics of the Møre Trøndelag Fault Complex, central Norway: constraints from new apatite fission track data. *Physics and Chemistry of the Earth, Parts A/B/C, 29*(10), 673-682. doi:https://doi.org/10.1016/j.pce.2004.03.005

Reston, T. J. (2009). The extension discrepancy and syn-rift subsidence deficit at rifted margins. *Petroleum Geoscience, 15*(3), 217-237. doi:doi:10.1144/1354-079309-845

Ribes, C., Manatschal, G., Ghienne, J.-F., Karner, G. D., Johnson, C. A., Figueredo, P. H., . . . Epin, M.-E. (2019). The syn-rift stratigraphic record across a fossil hyper-extended rifted margin: the example of the northwestern Adriatic margin exposed in the Central Alps. *International Journal of Earth Sciences, 108*(6), 2071-2095.

Richard, S. M., Smith, C. H., Kimbrough, D. L., Fitzgerald, P. G., Luyendyk, B. P., & McWilliams, M. O. (1994). Cooling history of the northern Ford Ranges, Marie Byrd Land, West Antarctica. *Tectonics, 13*(4), 837-857. doi:https://doi.org/10.1029/93TC03322

Seranne, M. (1992). Late Palaeozoic kinematics of the Møre-Trøndelag Fault Zone and adjacent areas, central Norway. *Norsk Geologisk Tidsskrift, 72*, 141-158.

Serck, C. S., Braathen, A., Hassaan, M., Faleide, J. I., Riber, L., Messager, G., & Midtkandal, I. (2022). From metamorphic core complex to crustal scale rollover: Post-Caledonian tectonic development of the Utsira High, North Sea. *Tectonophysics, 836*, 229416. doi:https://doi.org/10.1016/j.tecto.2022.229416

Serck, C. S., Braathen, A., Olaussen, S., Osmundsen, P. T., Midtkandal, I., van Yperen, A. E., & Indrevær, K. (2021). Supradetachment to rift basin transition recorded in continental to marine deposition; Paleogene Bandar Jissah Basin, NE Oman. *Basin Research, 33*(1), 544-569.

Steel, R. J., Næhle, S., Nilsen, H., Røe, S. L., & Spinnanger, A. (1977). Coarsening-upward cycles in the alluvium of Hornelen Basin (Devonian) Norway: Sedimentary response to tectonic events. *GSA Bulletin, 88*(8), 1124-1134. doi:10.1130/0016-7606(1977)88<1124:Ccitao>2.0.Co;2

Strugale, M., Schmitt, R. d. S., & Cartwright, J. (2021). Basement geology and its controls on the nucleation and growth of rift faults in the northern Campos Basin, offshore Brazil. *Basin Research, 33*(3), 1906-1933. doi:https://doi.org/10.1111/bre.12540

Sutra, E., & Manatschal, G. (2012). How does the continental crust thin in a hyperextended rifted margin? Insights from the Iberia margin. *Geology, 40*(2), 139-142.

Sutra, E., Manatschal, G., Mohn, G., & Unternehr, P. (2013). Quantification and restoration of extensional deformation along the Western Iberia and Newfoundland rifted margins. *Geochemistry, Geophysics, Geosystems, 14*(8), 2575-2597.

Tasrianto, R., & Escalona, A. (2015). Rift architecture of the Lofoten-Vesterålen margin, offshore Norway. *Marine and Petroleum Geology, 64*, 1-16.

Tugend, J., Manatschal, G., Kusznir, N. J., & Masini, E. (2015). Characterizing and identifying structural domains at rifted continental margins: application to the Bay of Biscay margins and its Western Pyrenean fossil remnants. *Geological Society, London, Special Publications, 413*(1), 171-203. doi:doi:10.1144/SP413.3

Vetti, V. V., & Fossen, H. (2012). Origin of contrasting Devonian supradetachment basin types in the Scandinavian Caledonides. *Geology, 40*(6), 571-574.

Welford, J. K., Peace, A. L., Geng, M., Dehler, S. A., & Dickie, K. (2018). Crustal structure of Baffin Bay from constrained three-dimensional gravity inversion and deformable plate tectonic models. *Geophysical Journal International, 214*(2), 1281-1300.

Welford, J. K., Shannon, P. M., O'Reilly, B. M., & Hall, J. (2010). Lithospheric density variations and Moho structure of the Irish Atlantic continental margin from constrained 3-D gravity inversion. *Geophysical Journal International, 183*(1), 79-95.

Wernicke, B. (1995). Low-angle normal faults and seismicity: A review. *Journal of Geophysical Research: Solid Earth, 100*(B10), 20159-20174. doi:https://doi.org/10.1029/95JB01911

Wernicke, B., & Axen, G. (1988). On the role of Isostasy in the Evolution of Normal-Fault Systems. *Geology, 16*. doi:10.1130/0091-7613(1988)016<0848:OTROII>2.3.CO;2

Whitney, D. L., Teyssier, C., Rey, P., & Buck, W. R. (2013). Continental and oceanic core complexes. *GSA Bulletin, 125*(3-4), 273-298. doi:10.1130/b30754.1

Wiest, J. D., Fossen, H., & Jacobs, J. (2020). Shear zone evolution during core complex exhumation – Implications for continental detachments. *Journal of Structural Geology, 140*, 104139. doi:https://doi.org/10.1016/j.jsg.2020.104139

Zalán, P. V., Severino, M. d. C., Rigoti, C. A., Magnavita, L. P., Oliveira, J. A. B., & Vianna, A. R. (2011). *An entirely new 3D-view of the crustal and mantle structure of a South Atlantic passive margin–Santos, Campos and Espírito Santo basins, Brazil.* Paper presented at the AAPG annual conference and Exhibition.

Zastrozhnov, D., Gernigon, L., Gogin, I., Planke, S., Abdelmalak, M. M., Polteau, S., . . . Myklebust, R. (2020). Regional structure and polyphased Cretaceous-Paleocene rift and basin development of the mid-Norwegian volcanic passive margin. *Marine and Petroleum Geology, 115*, 104269.

Figures

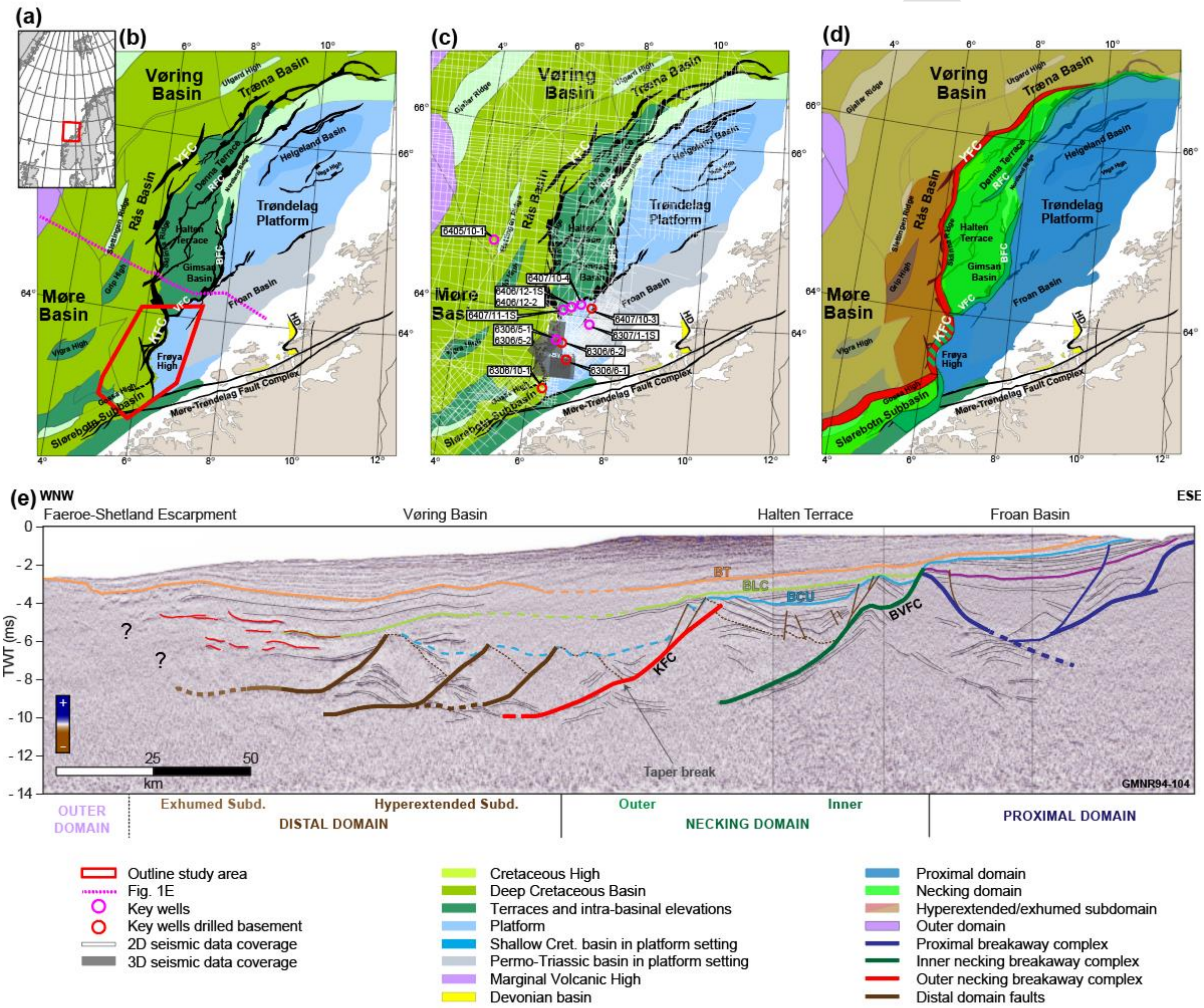

Figure 1) (a) Map of the northern North-East Atlantic with location of maps of the mid-Norwegian Rifted margin shown in b-d. (b) Proximal part of the Mid-Norwegian rifted margin with main tectonic elements and Late Jurassic fault polygons modified after Blystad et al. (1995) and Bunkholt et al. (2021). (c) Seismic and well data base map. (d) Map color-coded with rift domains and associated breakaway complexes (after Osmundsen & Péron-Pinvidic, 2018). (e) Regional geologic features interpreted on 2D seismic line GMNR94-104, see Figure 1b for location. Large-magnitude faults are color-coded based on their corresponding margin domain; blue: proximal; green and red; necking; brown; distal. Intrabasement reflectivity show domal culminations in the footwall segment of the large-magnitude faults, notably at successively lower crustal levels from the proximal to the distal domain. BCU: Base Cretaceous Unconformity; BLC: Base Late Cretaceous; BT: Base Tertiary;

BVFC: Bremstein-Vingleia Fault Complex; HD: Høybakken Detachment; KFC: Klakk Fault Complex; RFC: Revfallet Fault Complex; Subd.: subdomain; TWT: two-way time; VFC: Vingleia Fault Complex; YFC: Ytreholmen Fault Complex. Seismic data courtesy of NPD DISKOS NTNU Database.

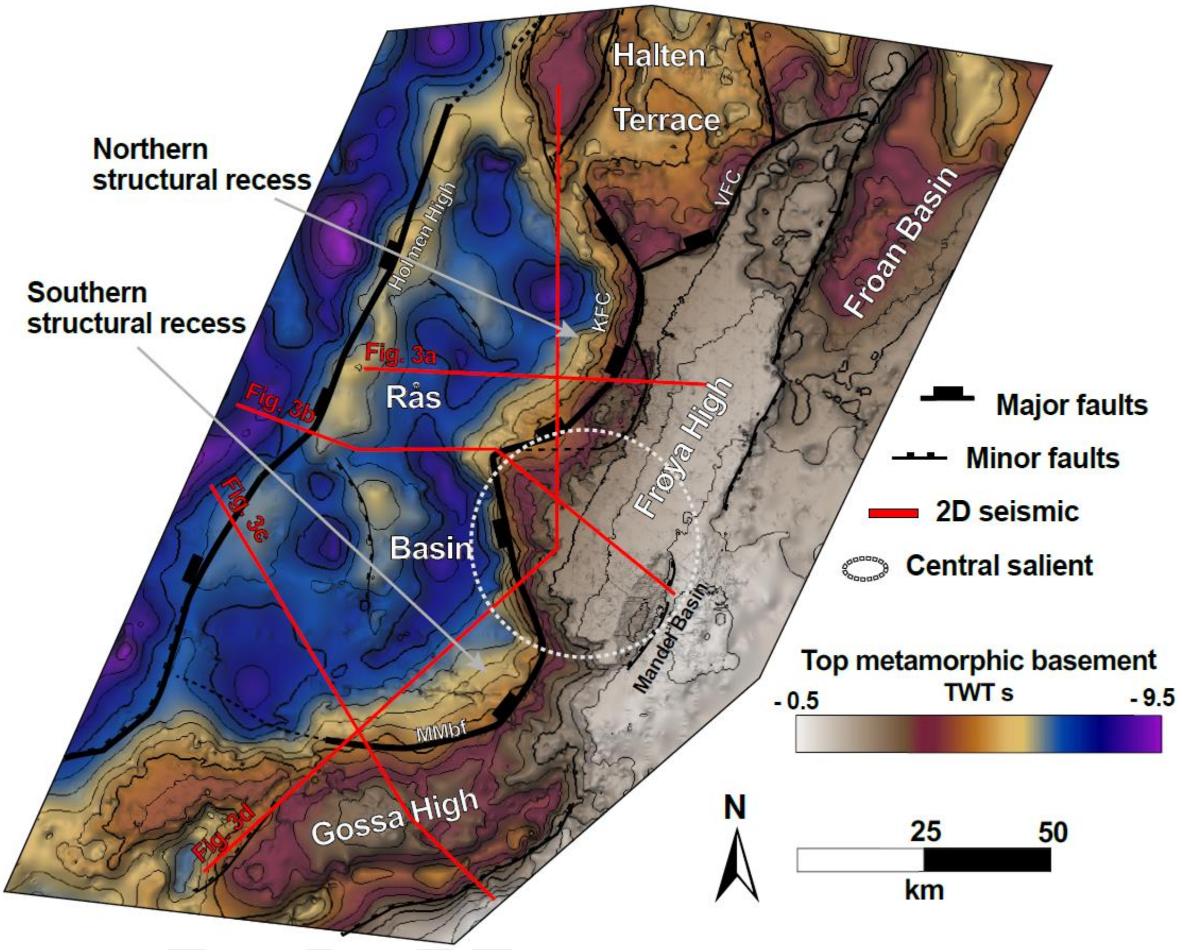

Figure 2) Time-structure map of top metamorphic basement within study area (Figure 1b for location) as mapped in seismic reflection data. Here shown with a 5-time vertical exaggeration. Red lines correspond to seismic sections in Figure 3. BVFC: Bremstein-Vingleia Fault Complex; KFC: Klakk Fault Complex; MMbf: Main Møre boundary fault; VFC: Vingleia Fault Complex.

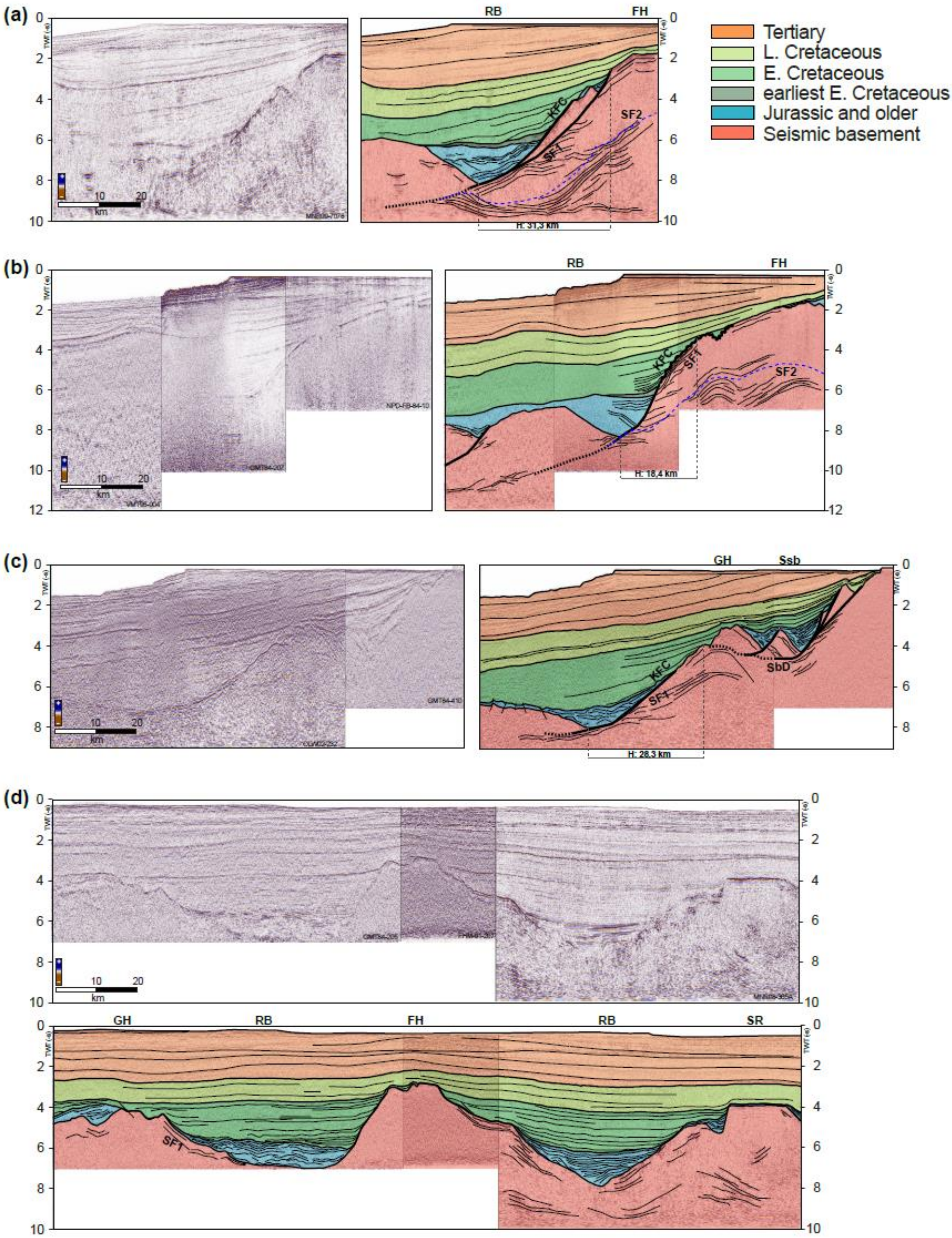

Figure 3) Seismic transects a-d, see Figure 2 for locations, without and with superimposed interpretations. (a) In the northern structural recess, a Jurassic basin rests upon a rider hangingwall block in the KFC. The Frøya High in the footwall has notably two planar erosional surfaces onlapped

by Late Cretaceous strata. The pre-Cretaceous strata shows a wedge-shaped geometry, with internal surfaces suspected to correspond to intra-basinal unconformities. (b) The central salient of the Frøya High shows a severely eroded fault scarp with a convex upwards shape of the both the footwall and SF2 internally. SF1 is observed in immediate proximity to the eroded KFC fault scarp. Early Cretaceous strata onlaps the Frøya High in its footwall. (c) Rotated fault blocks capped by pre-Cretaceous strata rest above the Slørebotn Detachment in the Slørebotn Subbasin. West of the Gossa High, the KFC partly reactivated and incised the interpreted western continuation of the Slørebotn detachment. (d) Along-strike of the KFC, pre-Cretaceous strata can be observed in the Rås Basin on both flanks of the Frøya High. RB: Rås Basin; FH: Frøya High; H: measured fault heave; KFC: Klakk Fault Complex; SR: Sklinna Ridge; GH: Gossa High: Ssb: Slørebotn Subbasin. SF1: seismic facies 1; SF2: seismic facies 2. Seismic data courtesy of NPD DISKOS NTNU Database.

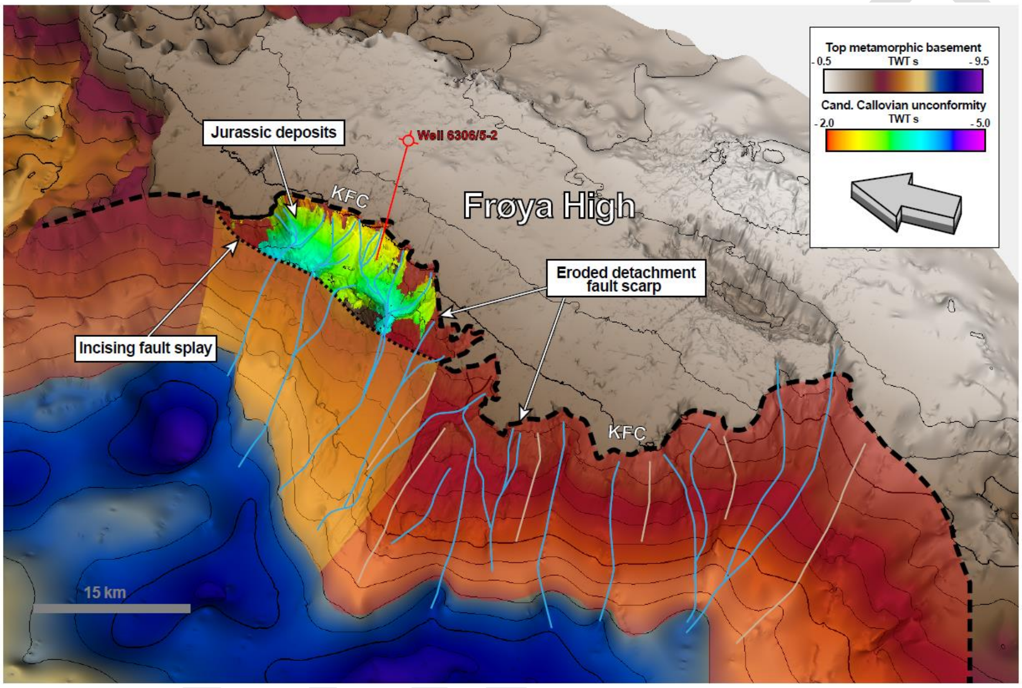

Figure 4) Time structure map of top metamorphic basement of the Frøya High in 3D (five times vertically exaggerated) with incising valleys and ridges indicated with blue and yellow lines, respectively. The eroded fault scarp of the main detachment for the KFC is colorcoded in red, younger fault splay colorcoded in yellow. Interpreted seismic reflection horizon of the Intra Melke Formation Sandstones (IMU) of candidate (Cand.) Callovian age as correlated with well 6306/5-2 is superimposed on the top metamorphic basement map above the rider fault block (see Figure 3a for corresponding geometry in cross-section). Notably, the IMU horizon also exhibits incising valleys, indicating sediment transport and erosion of Jurassic strata following deposition of late Middle Jurassic sediments. KFC: Klakk Fault Complex.

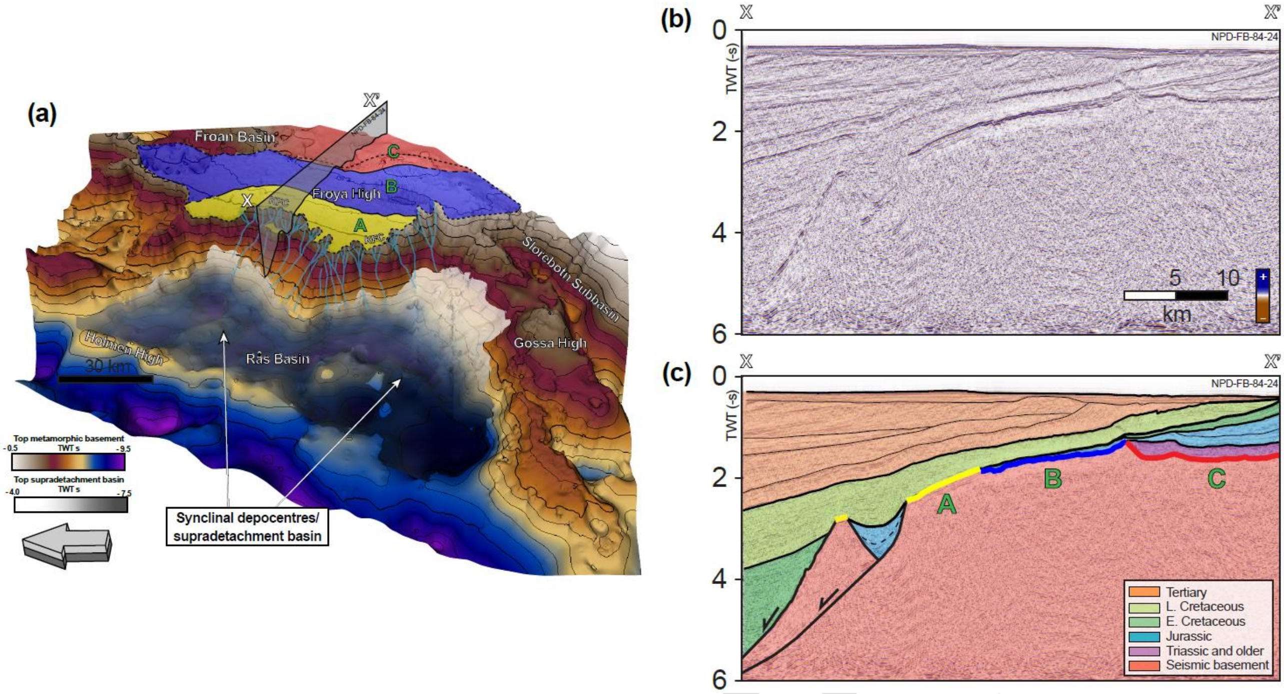

Figure 5) Time structure map of top metamorphic basement of study area in 3D, shown with five times vertical exaggeration (Figure 1 for location). Top supradetachment basin surface corresponds to Candidate Base Cretaceous. Blue lines indicate incising valleys and sediment pathways from footwall to hangingwall basin. Black stippled line outlines the Frøya High after Blystad et al. (1995). Top basement surface segments A (yellow), B (blue) and C (red), separated by different dips are superimposed. Their boundaries reflect transverse ridges across the high, and their trend roughly follow the strike of the KFC. (b) Seismic section X-X' without interpretation. (c) Seismic section X-X' with interpretation. Top basement segments A-C are indicated and color-coded as in (a). Note how the eroded top of the hangingwall rider block is included in basement segment A. Seismic data courtesy of NPD DISKOS NTNU Database.

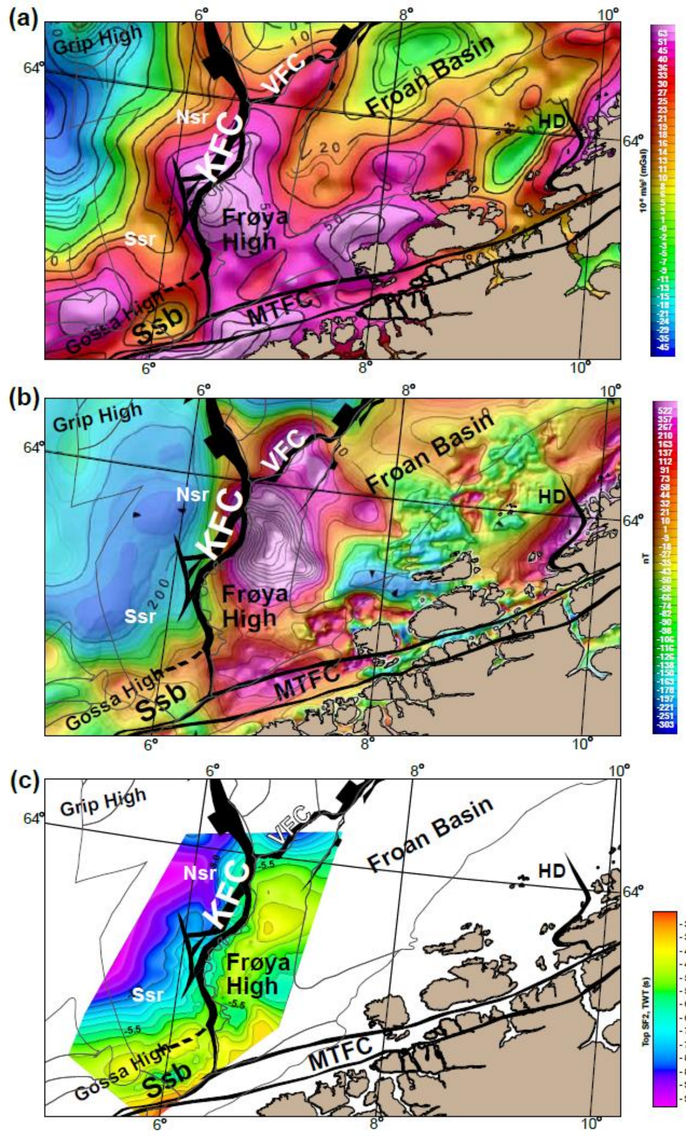

Figure 6) Maps over study area compiled and modified from Bunkholt et al. (2021); NPD (2022); Olesen et al. (2010a); Olesen et al. (2010b). (a) Gravity anomaly map (Olesen et al., 2010a). The displayed gravity anomalies are calculated as isostasy-corrected free-air anomalies using a rock density of 2670 kg/m3. The high gravity anomalies roughly coincide with the prevalence of the Frøya High basement terrain (see also Figure 2). (b) Magnetic anomaly map (Olesen et al., 2010b). The displayed magnetic anomalies have been extracted from total magnetic values using Definite Geomagnetic Reference Field (DGRF) on single grids. Relatively high anomaly values are recorded on the central part of the Frøya High and the highest values are observed between the central part of the Frøya High and the VFC. C) Compiled time-structure map for the study area of the intrabasement Seismic Facies 2 (SF2) horizon. In comparison with (b), the magnetic anomalies within the study area coincides with where the SF2 is mapped at relatively high structural levels; the central part of the high and in its transition towards the VFC. Abbreviations: HD: Høybakken Detachment; KFC: Klakk Fault Complex; MTFC: Møre-Trøndelag Fault Complex; Nsr: Northern structural recess; Ssb: Slørebotn Subbasin; Ssr: Southern structural recess; VFC: Vingleia Fault Complex.

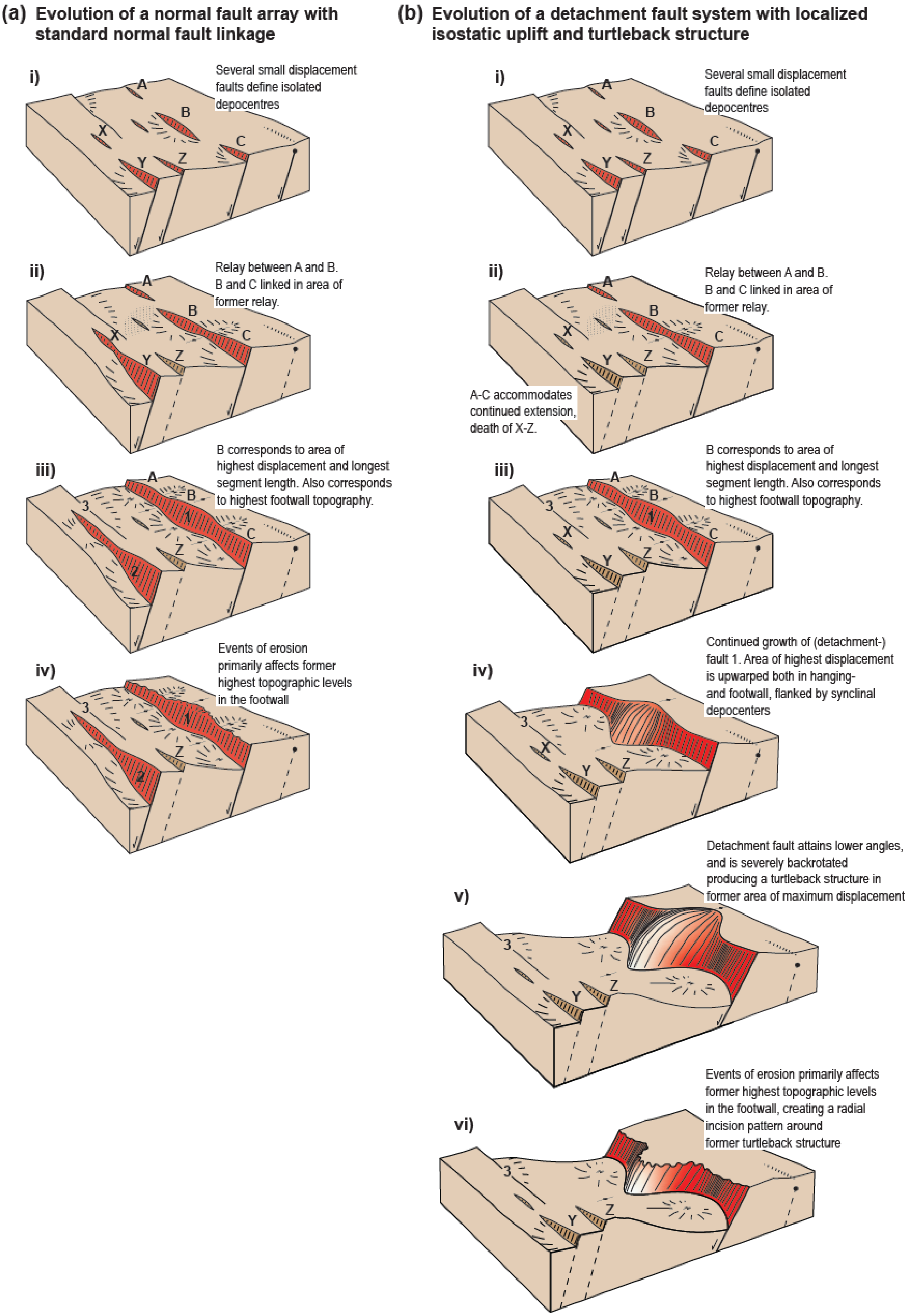
(a) Evolution of a normal fault array with standard normal fault linkage
i)
Several small displacement faults define isolated depocentres
A
B
X
C
Y
Z
ii)
Relay between A and B. B and C linked in area of former relay.
iii)
B corresponds to area of highest displacement and longest segment length. Also corresponds to highest footwall topography.
1
2
3
iv)
Events of erosion primarily affects former highest topographic levels in the footwall
(b) Evolution of a detachment fault system with localized isostatic uplift and turtleback structure
A-C accommodates continued extension, death of X-Z.
Continued growth of (detachment-) fault 1. Area of highest displacement is upwarped both in hanging- and footwall, flanked by synclinal depocenters
v)
Detachment fault attains lower angles, and is severely backrotated producing a turtleback structure in former area of maximum displacement
vi)
Events of erosion primarily affects former highest topographic levels in the footwall, creating a radial incision pattern around former turtleback structure

1217

Figure 7) Schematic 3D evolution of fault evolution during extension, with erosion of highest topography after rifting. The illustration is an attempt to summarize and implement the findings of previous publications schematically, including the works of Brun et al. (2018); Gawthorpe and Leeder (2000); Lavier et al. (1999), see text for further elaboration. Scale not implied. (a) The evolution of a normal fault array largely as outlined by Gawthorpe and Leeder (2000) with i) the initiation stage, characterized by numerous small displacement faults (faults A-C, X-Z) and isolated depocenters, ii) the interaction and linkage stage where deformation localizes between larger fault zones formed by linking of previously isolated fault segments, iii) the through-going fault stage, where continued linkage establishes major fault segments and associated depocenters in a typical hangingwall basin-setting, and iv) expected footwall erosion of the highest topography if stage (iii) marks the end of rifting and is followed by a base-level drop below extension induced footwall topography prior to significant post-rift system subsidence. Notably, footwall anticlines are most sensitive to erosion, but the overall strike of fault segment 1 remains largely intact. (b) The evolution of a detachment fault system during extension, assuming larger amounts of displacement and deformation localization along one major fault segment as typically reported from necking domains with i) the initiation stage showing the same configuration as for normal fault array systems (A), ii) the interaction and linkage stage where deformation localizes along one larger fault zone formed by linking of previously isolated fault segments B and C, while X-Z experiences no further displacement, iii) the through-going fault stage where continued linkage establishes a major fault segment and associated depocenters in a typical hangingwall basin-setting, iv) continued displacement along fault segment 1, illustrated to include the modelling results of Lavier et al. (1999), inferring a localized isostatic response in the area of most extension and longest segment length, effectively causing a basin inversion in the corresponding area in the hangingwall basin. Synclinal depocenters are established on the flanks of the exhumed and inverted fault plane, v) continued displacement along fault segment 1, illustrated to include the modelling results of Lavier et al. (1999) at c. 27 km displacement, inferring a full detachment fault plane backrotation and establishment of a turtleback structure in the area of most extension and longest segment length. This accentuates the basin inversion in the corresponding area in the hangingwall basin and further deepens the synclinal depocenters on the flanks of the exhumed turtleback, and vi) expected footwall erosion of the highest topography if stage (v) marks the end of rifting and is followed by a base-level drop below extension induced footwall topography prior to significant post-rift system subsidence. The detachment fault plane scarp exhibits a sinusoidal geometry with a radial erosional pattern sourced from the former highest footwall topography, in turn corresponding to the former hinge of the turtleback anticline structure.

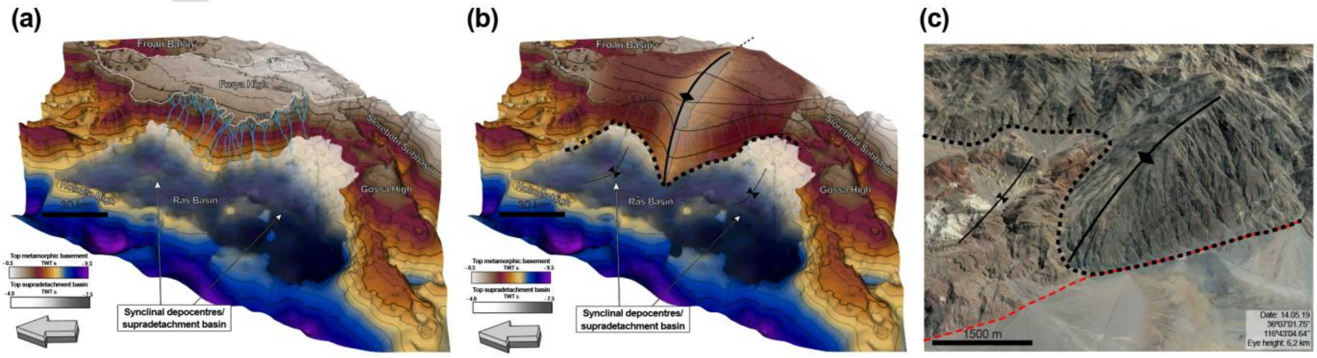

Figure 8) (a) Time structure map of top metamorphic basement of study area in 3D, shown with five times vertical exaggeration (Fig. 1 for location). White stippled line outlines the Frøya High after Blystad et al. (1995). Blue lines indicate incising valleys and sediment pathways from footwall to hangingwall basin. Top supradetachment basin surface corresponds to Candidate Base Cretaceous. (b) Same as (a), including detachment fault surface outline (black stippled line) and interpreted footwall turtleback geometry. Synclinal depocenters included in hangingwall supradetachment basin. (c) 3D map view of the Copper Canyon Turtleback, western US, with structural interpretations of detachment fault system anticlines and synclines superimposed. Black stippled line outlines the detachment fault (Miocene-Pliocene), red stippled line outlines partly reactivating normal fault (Holocene) after Miller and Pavlis (2005) and Knott et al. (2005) (Google Earth Google, 2022).

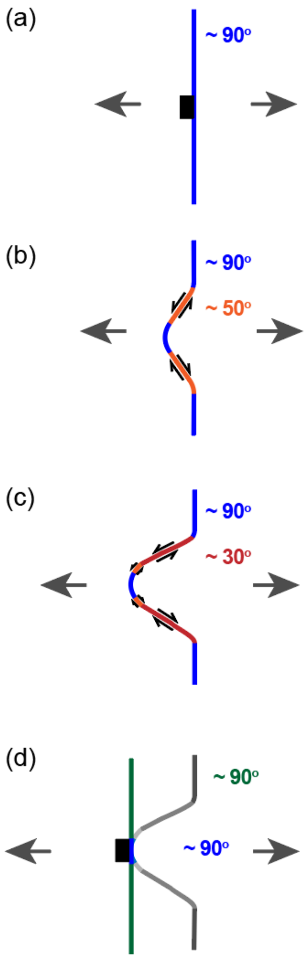

Figure 9) Conceptual sketch (scale not implied) displaying the evolution of shear stress along-strike of a normal detachment fault attaining an increasingly sinusoidal geometry during rifting. Direction of extension indicated with grey arrows. (a) normal fault initiation with overall fault strike developing at an ideal angle of 90 degrees, perpendicular to the direction of extension. (b) as sinuosity increases with detachment fault evolution, the flanks (orange) experiences increased shear stress. As illustrated here, the flanks likely experience oblique-slip movements where the angle between the fault plane and the direction of extension has decreased to c. 50°. (c) with increasing extension, sinuosity of the detachment fault plane also increases, effectively decreasing the angle between the direction of

extension and detachment fault plane, here illustrated at c. 30°. This likely motivates oblique-slip to strike-slip movements along the central salient flanks (red). (d) Conceptually, establishing new faults (green) at a higher angle to the direction of extension will prove more favorable than continued slip on the original detachment fault plane, of which parts may be abandoned. This will likely occur after a sufficient level of displacement and detachment fault geometry evolution governed by e.g., crustal rheology and effective stresses. Slip may still occur on the segments of the sinusoidal detachment fault plane which remain oriented at a high angle to the direction of extension. New fault segments may grow and link up with parts of the original detachment fault plane. Slip may thus continue on a fault surface consisting of both younger successive faults (green) and segments of the original detachment fault plane (blue). Notably, this concept entails that with ongoing extension and possible changes in strain field orientation, some segments of the detachment fault plane may be later reactivated if they become more favorably oriented relative to the strain field.